Post-drought Groundwater Storage Recovery in California's Central Valley

Sarfaraz Alam[1], Mekonnen Gebremichael[1], Zhaoxin Ban[2], Bridget R Scanlon[3], Gabriel Senay[4], Dennis P Lettenmaier[2,1]

[1]Department of Civil & Environmental Engineering, University of California, Los Angeles.
[2]Department of Geography, University of California, Los Angeles.
[3]Bureau of Economic Geology, Jackson School of Geosciences, The University of Texas at Austin.
[4]Earth Resources Observation and Science (EROS) Center, USGS, Fort Collins

Corresponding author: Sarfaraz Alam (szalam@ucla.edu)

Key Points:

- Groundwater storage recovery during post-drought periods ranged from 34% (2007–2009 drought) to 13% (2012–2016 drought).
- Projected drought recovery times decrease by a factor of 3.6-7.8 with post-drought periods containing a) no drought years or b) wet years only.
- Overdraft recovery times decrease ~2x with implementation of modest pumping restrictions under no-drought post-drought climate.

Abstract

Groundwater depletion is a major threat to agricultural and municipal water supply in California's Central Valley. Recent droughts during 2007–2009 and 2012–2016 exacerbated chronic groundwater depletion. However, it is unclear how much groundwater storage recovered from drought-related overdrafts during post-drought years, and how climatic conditions and water management affected recovery times. We estimated groundwater storage change in the Central Valley for April 2002 through September 2019 using four methods: GRACE satellite data, a water balance approach, a hydrologic simulation model, and monitoring wells. We also evaluated the sensitivity of drought recovery to different climate scenarios (recent climate ± droughts) and future climate change scenarios (20 GCMs and 2 RCPs). Central Valley groundwater loss ranged from 19 km^3 (2007 – 2009) to 26 km^3 (2012 – 2016) (median of four methods). Aquifer storage recovery was 34% and 13% of the overdraft during the 2010–2011 and 2017–2019 post-drought years. Numerical experiments show that recovery times are sensitive to

climate forcing, with longer recovery times for a future climate scenario that replicates historical climatology relative to historical forcing with no-drought. Recovery times for groundwater pumping restrictions at 30th to 50th percentiles of historic groundwater depletion were reduced by ~2× relative to no pumping restrictions under no-drought future climatology. This study highlights the importance of considering water management within the context of climate change scenarios to determine future drought recoveries.

Plain language summary:

California's Central Valley has experienced chronic groundwater depletion over the past few decades, the rate of which has been amplified by droughts in 2007-2009 and 2012-2016. There is limited knowledge as to how much of the drought-caused groundwater depletion has recovered during post-drought years and how climate and water management affect overdraft recovery times. We address these issues by estimating groundwater storage changes using four methods and conducting numerical experiments with varying climatic conditions and water management options. We find that less than one-third of the groundwater overdraft from the most recent droughts was recovered during post-drought years. Projected overdraft recovery times vary greatly depending on the climate scenarios and water management strategies, and future droughts are likely to cause overdrafts from which recovery is unlikely given the current level of groundwater extractions. However, management measures such as capping groundwater pumping could reduce recovery times by a factor of two or more depending on the groundwater extraction cap and post-drought climate.

1 Introduction

Groundwater overdraft during droughts is common in semiarid regions globally (Wada et al., 2010), and climate change is expected to further accelerate groundwater depletion in these regions (Alam et al., 2019; Wu et al., 2020). Groundwater overdrafts linked to droughts are caused both by reduced groundwater recharge and increased agricultural, industrial, and municipal water demand (Russo and Lall, 2017; Taylor et al., 2013). The impact of drought on groundwater can be especially severe in irrigated agricultural regions with limited surface water supply. There is a critical need to understand drought impacts on groundwater and to identify measures to improve resiliency to droughts (Taylor et al., 2013).

Recovery of groundwater is critical for long term environmental and agricultural sustainability. However, aquifers in semi-arid regions such as the U.S. High Plains and northeastern India have shown limited resilience to drought events — the groundwater depletion during droughts are typically not fully recovered (Famiglietti et al., 2011; Rodell and Famiglietti, 2002; Scanlon et al., 2012; Voss et al., 2015). Limited recovery can be attributed to excess groundwater use that in some regions exceeds the net volume of water supplied during wet post-drought years. For instance, groundwater in the Central and Southern High Plain aquifers (USA) has been declining over the past few decades (39 km^3 during 2002 to 2017), and there has been very low overdraft recovery during this time (i.e., 2006 through 2010) (Rateb et al., 2020). In contrast, there are also some regions that show rapid groundwater recovery during post-drought years (e.g., Texas Gulf Coast) (Rateb et al., 2020). Irrespective of the recovery pattern (rapid vs slow), precipitation and related surface water supply are key to overdraft recovery as high precipitation promotes greater groundwater recovery. Additionally, precipitation events affected by large scale climatic conditions, such as the El Niño Southern Oscillation (ENSO) (2 to 7-year cycle) or the North Atlantic Oscillation (NAO) (3 to 6-year cycle) have been found to influence groundwater level variability in many aquifers globally, e.g., North Atlantic Coastal Plain principal aquifers (USA), Northwest India, Southwest British Columbia and other regions (Asoka et al., 2017; Fleming and Quilty, 2006; Kuss and Gurdak, 2014; Perez-Valdivia et al., 2012). However, the complex interplay between climatic conditions (e.g., precipitation) and the nature of groundwater recovery is modulated by water management (e.g., groundwater pumping,

reservoir regulation), and varying hydrogeologic conditions. To our knowledge, there is no study that investigates the groundwater recovery associated with droughts and its connection to precipitation and water management practices, particularly in highly managed aquifer (e.g., Central Valley of California).

California's Central Valley (CV)—one of the richest agricultural regions in the world—has experienced frequent droughts over the past half century, with the last decade marked by two major drought periods: 2007–2009 and 2012–2016 (Famiglietti, 2014; Faunt et al., 2016; Thomas et al., 2017). Despite the droughts, agricultural water consumption in the CV did not decrease during the drought years (Alam et al., 2019a; Gebremichael et al., 2021). The effects of drought instead were mitigated by supplementing or replacing surface water supply sources with groundwater (Famiglietti et al., 2011; Ralph & Dettinger, 2012). Increased water demand over time compounded by ongoing climate change have resulted in long-term groundwater depletion in the CV, which was accelerated during the 2007–2009 and 2012–2016 droughts (CDWR, 2013; Hanak et al., 2017; Xiao et al., 2017). The historic chronic groundwater depletion (Faunt et al., 2009) motivated the State Legislature to enact the Sustainable Groundwater Management Act (SGMA), which mandates sustainable groundwater use (California State Legislature, 2014). While the use of groundwater to mitigate surface water shortages during droughts may be an obvious management response that improves the reliability and robustness of the system, post-drought recovery of groundwater overdraft is key to long-term sustainability. To ensure post-drought groundwater storage recovery and develop a sustainable groundwater management plan that increases groundwater resilience, there is a critical need for improved understanding of (1) how much groundwater was recovered during post-drought years, and (2) the influence of climate vs anthropogenic factors on post-drought groundwater recovery.

A major constraint in understanding post-drought groundwater recovery is the lack of reliable groundwater storage data on a regional scale. Groundwater storage change estimates for the CV vary substantially among different methods (Alam et al., 2020; Ojha et al., 2020; Scanlon, et al., 2012), and this has made understanding of drought recovery challenging. Commonly used methods for groundwater storage change estimation are, (1) well measurements (Rateb et al., 2020; Scanlon et al., 2012), (2) Gravity Recovery and Climate Experiment (GRACE) satellite-based estimates (Rateb et al., 2020; Scanlon et al., 2012), (3) water balance

methods (Xiao et al., 2017), and (4) hydrologic simulation models (Brush, 2013; Faunt et al., 2016). Each of these methods has its own strengths and weaknesses. Well data provide direct measurements of groundwater levels, yet such measurements are scarce in many places, lack continuous long-term measurements, and calculation of groundwater storage from well measurements is prone to large uncertainties because of lack of knowledge of aquifer storage coefficients and order of magnitude variations in storage coefficients between unconfined and confined aquifers. Continuous estimates of groundwater storage change (2002 to present) can be derived from the GRACE satellites which measure terrestrial water storage (TWS); however, the GRACE footprint is large (~150,000 km^2), limiting small scale groundwater storage change estimation (Long et al., 2016; Longuevergne et al., 2007). Another approach to estimate regional groundwater storage change is through the water balance method (WB), which sums the influxes (precipitation, inflow) and subtracts the outfluxes/storage changes (evapotranspiration [ET], outflow, in soil moisture, snow, and surface water) over a prescribed domain (Xiao et al., 2017), closes the water balance (and hence provides groundwater storage change estimates compatible with the other hydrological components), yet it is subject to estimation errors from each of the water balance components. Hydrologic models simulate continuous groundwater storage changes, and are ideal to perform scenario experiments (Dogrul et al., 2016; Faunt et al., 2016). However, such simulations are subject to errors resulting from model's approximation to physical process, parameter estimation, and input data accuracy.

In summary, each of the groundwater storage change estimation/measurement methods has its own pros and cons, and there is no single method that is likely to outperform others. Past studies of groundwater change in the CV (and many other regions of the world) have relied on only one or two of the above methods. For instance, Xiao et al. (2017) estimated groundwater depletion and post-drought recovery for the 2007–2009 drought using GRACE satellite data and the WB method. They found groundwater depletion trends for the two methods were similar, but recovery rates differed substantially. We argue that in order to fully understand post-drought groundwater storage recovery, it is important to formally acknowledge differences in results from the various groundwater estimation methods, but to use multiple methods to the maximum extent possible. This can be done through the use of all available groundwater estimation methods and by identifying and acknowledging agreements and disagreements in the results. To

our knowledge, no study has been performed on CV that examines and compares groundwater depletion and recovery rates from all four-groundwater storage change estimation methods.

Climate and anthropogenic factors can strongly influence groundwater depletion and recovery (Alam, et al. 2019; Hanson et al. 2012; Taylor et al. 2013; Wu et al. 2020). Droughts cause groundwater depletion; the drought recovery period is often calculated from post-drought precipitation duration and magnitude (DeChant and Moradkhani, 2015; Pan et al., 2013). High precipitation during post-drought years reduces post-drought recovery period, but the effective recovery rate may be hindered by anthropogenic factors, such as increased agricultural and municipal groundwater pumping (Gleeson et al., 2012; Ojha et al., 2020). Although drought impacts on groundwater availability have been well studied (Argus et al. 2017; Scanlon et al. 2012; Taylor et al. 2013; Thomas and Famiglietti 2019; Xiao et al. 2017), it is unknown how groundwater recovery during post-drought years relates to post-drought precipitation. In addition to degree of recovery of groundwater storage, the rate at which groundwater recovery occurs is a key indicator of the resilience of the groundwater system. Rapid recovery indicates that an aquifer is resilient to extreme climate conditions such as drought. In contrast, slow recovery can be threatening as another drought event may begin before full recovery from a previous drought. In the past few decades, there were a few wet spells over California, but it is unknown if such wet spells are sufficient for recovery of groundwater overdraft during droughts, and if not, what measures could be implemented to assure full post-drought groundwater overdraft recovery. The overdraft recovery duration and its relationship with precipitation amount in the CV aquifer is currently unknown.

The objective of this study is to address the following questions: (1) how much of the groundwater storage overdraft related to recent droughts in the CV was recovered during post-drought years? and (2) what is the role of precipitation and water management strategies in rapid versus slow post-drought groundwater storage recovery? We address these issues using the four methods summarized previously. We also isolate the impact of future climate on groundwater storage recovery from drought using different scenarios (historical climatology, no drought, wet years only) and climate change impacts using 20 Global Climate Models (GCMs) and two Representative Concentration Pathways (RCPs) from the IPCC Fifth Assessment Report. Our

outcomes are intended to provide insights into drought resiliency that could help in developing groundwater management plans mandated by SGMA (California State Legislature, 2014).

2 Study area

The CV, located along a north-south transect in California, drains three major watersheds that deliver water to the CV region: the Sacramento, San Joaquin, and Tulare (SSJT watersheds) (Figure 1a). The CV is a flat valley of about 54,000 km^2 area surrounded by mountains: the Sierra Nevada to the east and the Coastal range to the west. The climate of this region is Mediterranean, with most precipitation occurring in the winter (November through March), out of phase with evaporative demand which is high in the summer (July through September) (Cooper et al., 2018). The two major droughts of the past two decades (2007–2009 and 2012–2016) resulted in 38.6% of California being in severe to exceptional drought categories (according to the U.S. Drought Monitor) between 2007–2009, and 68% between 2012–2016, suggesting 2012–2016 drought was relatively more severe. See supporting information (SI), Figure S1.

Precipitation generally decreases both from north to south and through headwaters along valley to mountain transects (Figure 1a). Generally, headwater watersheds are considerably wetter than valley bottoms. About half (~28,000 km^2) of the CV is irrigated. The source of water is a mixture of surface and groundwater (Hanak, 2011). The contrast in north-south water demand and supply motivated the construction of headwater reservoirs and infrastructure that convey surface water from the Sacramento-San Joaquin River Delta in the north to the south with infrastructure known as the State Water Project (SWP) and the federal Central Valley Project (CVP). Most of the surface water supply to the CV is generated in the headwater watersheds. More than 50 reservoirs (20 reservoirs in the Central Valley Project and 34 in the State Water Project) regulate inflows from the headwaters to the CV (CDWR, 2014; USBR, 2014). Surface water from headwater watersheds enters the CV at ~50 locations (Figure 1b). Excess surface water after meeting all demands (agricultural, municipal, and industrial) is released to the San Francisco Bay via the Delta.

The CV aquifer contains unconsolidated sedimentary deposits in stream channels, alluvial fans, and flood plains (Farrar and Bertoldi, 1988). The aquifer material in the western

CV (coastal) is relatively fine grained whereas the material in the eastern CV is much coarser grained (granite and volcanic). Lenses and beds of fine-grained material (Corcoran clay) are found predominantly in the southern Tulare Basin and the western San Joaquin Basin, and restrict vertical flow of groundwater (Planert and Williams, 1995).

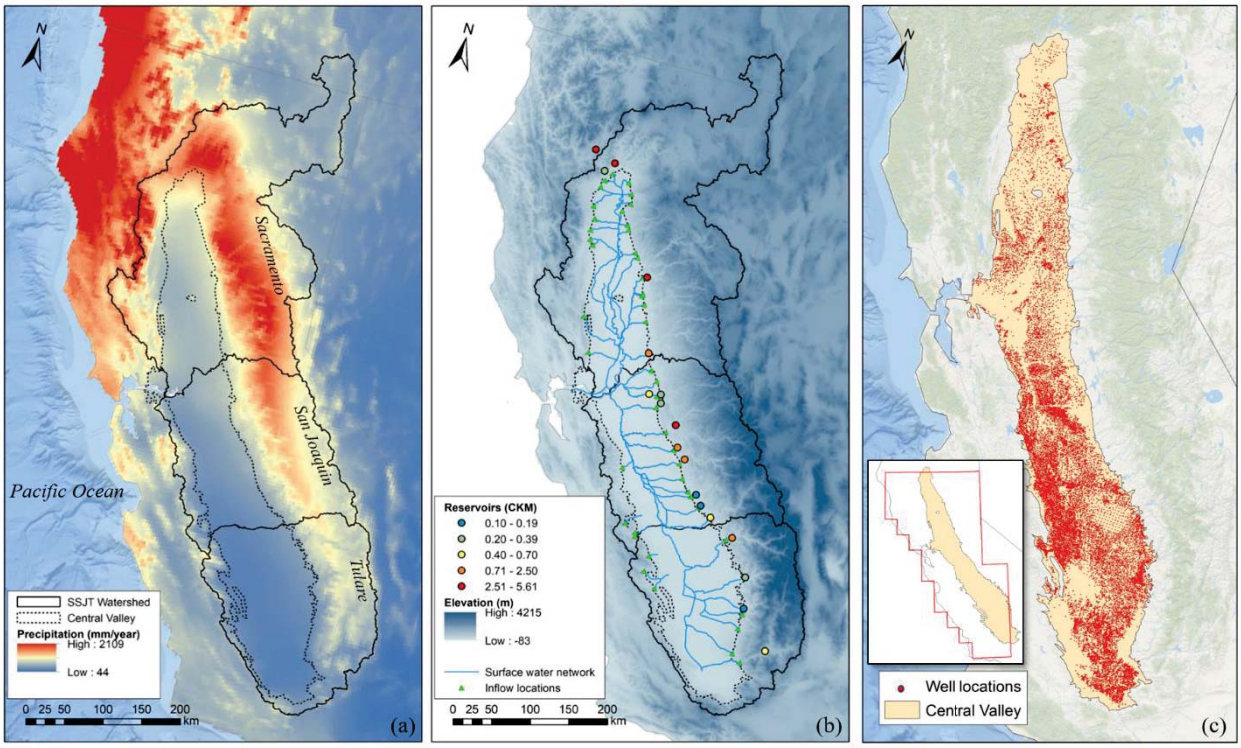

Figure 1. Study area: (a) Central Valley boundary and Sacramento-San Joaquin-Tulare (SSJT) watersheds, with long term mean annual precipitation (averaged over 2000-2018; source http://worldclim.org/); (b) Locations of major reservoirs (CDEC, 2020), with elevation, surface water network, and inflow locations to the CV; (c) Location of groundwater wells (total 23,048) in the CV (CASGEM, 2021). The inset in Figure 1c shows the GRACE analysis region (red border).

3 Data and Method

We produced multiple estimates of groundwater storage (GWS) change and conducted numerical experiments to quantify the role of climate and water management on groundwater overdraft recovery following drought. Our approach follows three steps:

(1) Estimate GWS changes using four different methods,

(2) Conduct numerical experiments with different climatic conditions and water management options to estimate the time for GWS recovery from drought,

(3) Conduct numerical experiments to estimate the time for GWS recovery under future climate change.

In Step (1), we estimated GWS changes using the four methods: GRACE satellite data, WB, model simulation, and well measurements. In Steps (2) and (3), we performed numerical experiments.

3.1 Metrics for measuring post-drought groundwater storage recovery

Metrics for estimating groundwater storage recovery time and volume following drought can take multiple forms. For instance, groundwater recovery can be measured with respect to the historical average condition or some other threshold level. In our case, we measure the post-drought groundwater recovery with respect to the pre-drought GWS level (see Figure S6, SI for detail). We used the following metrics for measuring recovery: GWS recovery volume (ΔGWS_{recov}), GWS depleted during drought ($\Delta GWS_{drought}$), GWS recovery percentage $\left(R_f\right)$, and GWS recovery duration (D_{rec}):

$$\Delta GWS_{recov} = GWS_{post\_drought} - GWS_{drought\_end} \quad (1)$$

$$\Delta GWS_{drought} = GWS_{drought\_end} - GWS_{drought\_start} \quad (2)$$

$$R_f = \frac{\Delta GWS_{recov}}{|\Delta GW_{drought}|} \times 100\% \quad (3)$$

$$D_{recov} = t_{post\_drought} - t_{drought\_end} \quad (4)$$

Where, D_{recov} is the time in months between the drought ending month ($t_{drought\_end}$) and the post drought month under consideration ($t_{post\_drought}$).

3.2 GWS change estimation using multiple methods in the recent decades

In order to characterize GWS depletion and recovery in the recent decade (2003–2019), we used GWS estimates made by four different methods. The GWS change estimation methods considered in this study are: (1) GRACE, (2) Wells, (3) WB, and (4) hydrologic model simulation (C2VSIM). The key input datasets used in each method are listed in Table 1.

247 **Table 1.** List of datasets used for estimating GWS change.

Data type	Data source	Spatial distribution/ resolution	Reference/note
Groundwater level	California Statewide Groundwater Elevation Monitoring (CASGEM)	Total stations in CV: 23,048	CASGEM (2021)
Terrestrial Total Water Storage Anomaly (TWSA)	GRACE and GRACE-FO MasCon. Two sources: (1) Jet Propulsion Laboratory (JPL-m) and (2) Center of Space Research (CSR-m)	0.5 degree	Save (2020); Save (2016); Watkins et al. (2015)
Reservoir storage	California Data Exchange Center	~50 reservoirs	CDEC (2020)
Streamflow	Inflow data from United States Geological Survey (USGS); outflow data from Dayflow	52 inflow locations and delta outflow	CDWR (2020); Dayflow (2020); USGS (2020)
Land use	USDA National Agricultural Statistics Service Cropland Data Layer	30 m	USDA-NASS (2020)
Precipitation	PRISM DAYMET Livneh et al. (L13)	4 km 1 km ~6 km (1/16th degree)	Daly et al. (2008) Thornton et al. (2017) Livneh et al. (2013)
Evapotranspiration, snow water equivalent, and soil moisture	Variable Infiltration Capacity (VIC) simulations	~6 km (1/16th degree)	VIC-4.1.2.g model simulated for this study
C2VSIM-FG simulated GWS	GWS obtained from C2VSIM simulation (2002-2015). We extended the simulation to September-2019.	Central Valley-wide	CDWR (2020)
Specific yield (Sy)	C2VSIM-FG model field CVHM model field	~1.65 km^2 (avg.) FE cells 1.61 km FD grids	CDWR (2020) Faunt et al. (2009)

248

249 ### *3.2.1 GRACE-based estimate of GWS change*

250 We used GRACE/GRACE-FO release (RL06) level 3 mass concentration (MasCon)
251 solutions from two sources, NASA Jet Propulsion Laboratory (JPL-m) and University of Texas
252 Center for Space Research (CSR-m). In contrast to the traditional processing method (i.e.,
253 spherical harmonics) (Bettadpur, 2012; Wahr et al., 1998), MasCon solutions can be applied at

regional scale as they better distinguish land and ocean signals, thus reducing leakage errors (reducing leakage of signal from land to ocean) (Long et al., 2016). Also constraining MasCon solutions with geophysical data during processing makes it suitable for the non-geodetic community. MasCon solutions parameterize the gravity field with regional concentration functions and have been applied globally in numerous studies (Save et al., 2016; Scanlon et al., 2016; Watkins et al., 2015). CSR and JPL MasCon solutions vary in the scale of grid cells; CSR uses ~1° (or ~120 km at the equator) hexagonal tiles of geodesic equal area (Save et al., 2016), and JPL solves the gravity field at a 3° spherical cap (~330 km at the equator) (Watkins et al., 2015). Details about CSR and JPL MasCon data processing are provided by Save et al. (2016) and Watkins et al. (2015).

We used the GRACE/GRACE-FO data for the period April-2002 through September-2019 to estimate GWS changes. The GRACE/GRACE-FO data provide the total water storage (TWS) anomaly at monthly time steps. TWS includes storages in snow, surface reservoir, soil moisture, and groundwater. We subtracted all of the storage terms from the TWS measurement to estimate the GWS change time series (see SI, Text S1 for detail). Because the GWS change in the CV (Figure 1a) is higher than that in the surrounding region (Xiao et al., 2017), we used the original 3-degree mascon tiles following (Ojha et al., 2019) to conduct an analysis that takes into account the groundwater signal potentially distributed inside each mascon tile. Figure 1c shows the GRACE analysis region (hereafter, we refer to GWS change in the GRACE analysis region as the change in the CV for GRACE/GRACE-FO based calculations). The GRACE/GRACE-FO based GWS change (ΔGWS) is computed by subtracting the soil moisture storage anomaly (ΔSMA), snow water equivalent anomaly ($\Delta SWEA$), and surface water storage anomaly ($\Delta SWSA$) from the terrestrial water storage anomaly ($\Delta TWSA$) obtained from JPL-m and CSR-m dataset:

$$\Delta GWS = \Delta TWSA - \Delta SMSA - \Delta SWEA - \Delta SWSA \qquad (5)$$

3.2.2 Water balance method

ΔGWS was estimated as a residual in the WB method. The WB components are precipitation, ET, storage changes (soil moisture, snow water equivalent, reservoir storage), streamflow into and out of the CV:

$$\Delta GWS = P + Q_{in} - Q_{out} - \Delta SMS - \Delta SWE - ET - \Delta SWS \quad (6)$$

where P, Q_{in}, Q_{out}, and ET are precipitation, surface water inflow to the CV, delta outflow from the CV and ET. ΔGWS, ΔSMS, ΔSWE and ΔSWS are changes in GWS, soil moisture storage, snow water equivalent and surface water storage (reservoirs), respectively. Table 1 provides a summary of data type, sources, and references (detailed descriptions in SI, Text S1).

3.2.3 Model simulations (C2VSIM)

We used an integrated groundwater-surface water simulation model, known as California Central Valley Surface-Groundwater Simulation Model (C2VSIM), to estimate GWS change for 2002 through 2019. C2VSIM, developed by California Department of Water Resources (CDWR), simulates all important hydrologic processes including streamflow, surface runoff, root-zone and vadose zone processes and groundwater flow (Brush, 2013; Dogrul et al., 2015). Its core is a finite element solver of the groundwater flow equations for finite element grids. Several previous studies have used the model to simulate groundwater-surface water dynamics in the CV region (Alam et al., 2020; Brush, 2013; Ghasemizade et al., 2019; Kourakos et al., 2019; Miller et al., 2009). The model is available at https://data.cnra.ca.gov/dataset/c2vsimfg-version-1-0 (last accessed: March 2021). We used version 1.0 of the C2VSIM fine grid model (IWFM-2015 version), which is the most updated version of the model (hereafter, referred as C2VSIM) (CDWR, 2020; See SI ,Text S3 and S4 for more detail).

3.2.4 GWS change calculation using well-measurements

We calculated GWS changes for the entire CV using groundwater head time series obtained from wells. We assembled groundwater level data from CDWR for 2002 through 2019 (CASGEM, 2021). There are 43,987 wells in the CASGEM database with multiple purposes (irrigation, domestic, monitoring, and others), including 23,014 groundwater wells are located in CV (Figure 1c). However, well records are not continuous at most locations and records are missing in many months. In general, the highest number of records are available for March and October (see SI, Figure S2, S3 for well numbers).

We computed volumetric GWS changes as the product of groundwater level changes, CV area, and storage coefficient (i.e., volume of water released from aquifer per unit decrease in head). Both groundwater level changes and the storage coefficient are uncertain. Groundwater level measurements from observation wells are generally a preferred option for calculating GWS changes, however, observation wells in CV are sparse in places, the number of measurements is below 500 in most of the months, and measurements are discontinuous. In contrast, there are numerous head measurements from pumping wells (e.g., well used for irrigation, industrial, residential, and other sectors), but they are pumped, which is reflected in the associated groundwater levels. That said, drawdowns due to pumping are expected to be small in winter, offering the possibility of the selective use of pumped wells.

Another complication is that there is limited knowledge of the storage coefficient in CV that is required to compute GWS from head change. There are stacked unconfined and confined aquifers within the CV. For unconfined aquifers the storage coefficient is the specific yield (Sy) - the volume of water released due to drainage from an unconfined aquifer per unit decline in groundwater level. In the CV, typical values range from 0.06-0.3 (Faunt et al., 2009). The storage coefficient in confined aquifers is typically 2 – 3 orders of magnitude less than that in unconfined aquifers (Faunt, 2009). In the unconfined aquifers, the groundwater surface (water table) is at atmospheric pressure and it declines as water drains through the porous media. In contrast, confined aquifers are bounded by an impermeable capping layer and groundwater is under pressures exceeding one atmosphere. Because the actual storage coefficient (both confined and unconfined) in the CV is unknown and there is limited knowledge of how much groundwater being extracted from unconfined versus confined aquifers, we used multiple storage coefficients and compare GWS estimation with other methods to obtain a sense of GWS trend and variability (more information in SI, Text S5).

We followed four steps to estimate GWS changes from well data: (1) spatial interpolation of groundwater levels using Inverse Distance Weighing (GWL, 10 km resolution) for each month from 2002 through 2019; (2) calculation of the month-to-month changes in GWL for each grid cell; (3) multiplication of GWL changes by storage coefficients and area to obtain volumetric GWS changes; (4) calculation the cumulative GWS changes. Similar to Scanlon et al. (2012), we added a 2% uncertainty to our estimates to account for errors associated with

interpolation. To identify suitable sets of well data capable of representing CV GWS changes, we generated two monthly GWS time series using: (1) only observation wells, (2) all types of wells (observation and pumped)

3.3 Numerical experiment for estimating groundwater recovery under multiple climate and water management scenarios

We conducted numerical experiments to quantify the recovery time for drought-associated groundwater overdraft for multiple droughts, recovery percentage, water management, and climatic conditions. Among the four GWS change estimates discussed earlier, we used WB method for numerical experiment as it is computationally efficient for a very large numbers of iterations necessary for this study. In order to consider a range of post-drought climate scenarios, we performed sampling experiment from past climate data that could represent the following scenarios:

- Recent climatology (2003–2019): Sampling of WB components from this period represents recent-decade climatology that includes different types of years (e.g., droughts 2007–2009, 2012–2016; wet years: 2011, 2017 and others)
- Long-term climatology (1982–2019): Sampling of WB components from this period represents long-term climatology.
- No-drought climatology (2003–2006, 2010–2011, 2017, 2019): Sampling of WB components from this period represents optimistic scenario where droughts do not occur.
- Wet climatology (2005-2006, 2011, 2017, 2019): Sampling of monthly WB components from this period represents wet climatic condition where Standardized Precipitation Index exceeds 0.5. This scenario provides an upper bound for the GWS recovery.

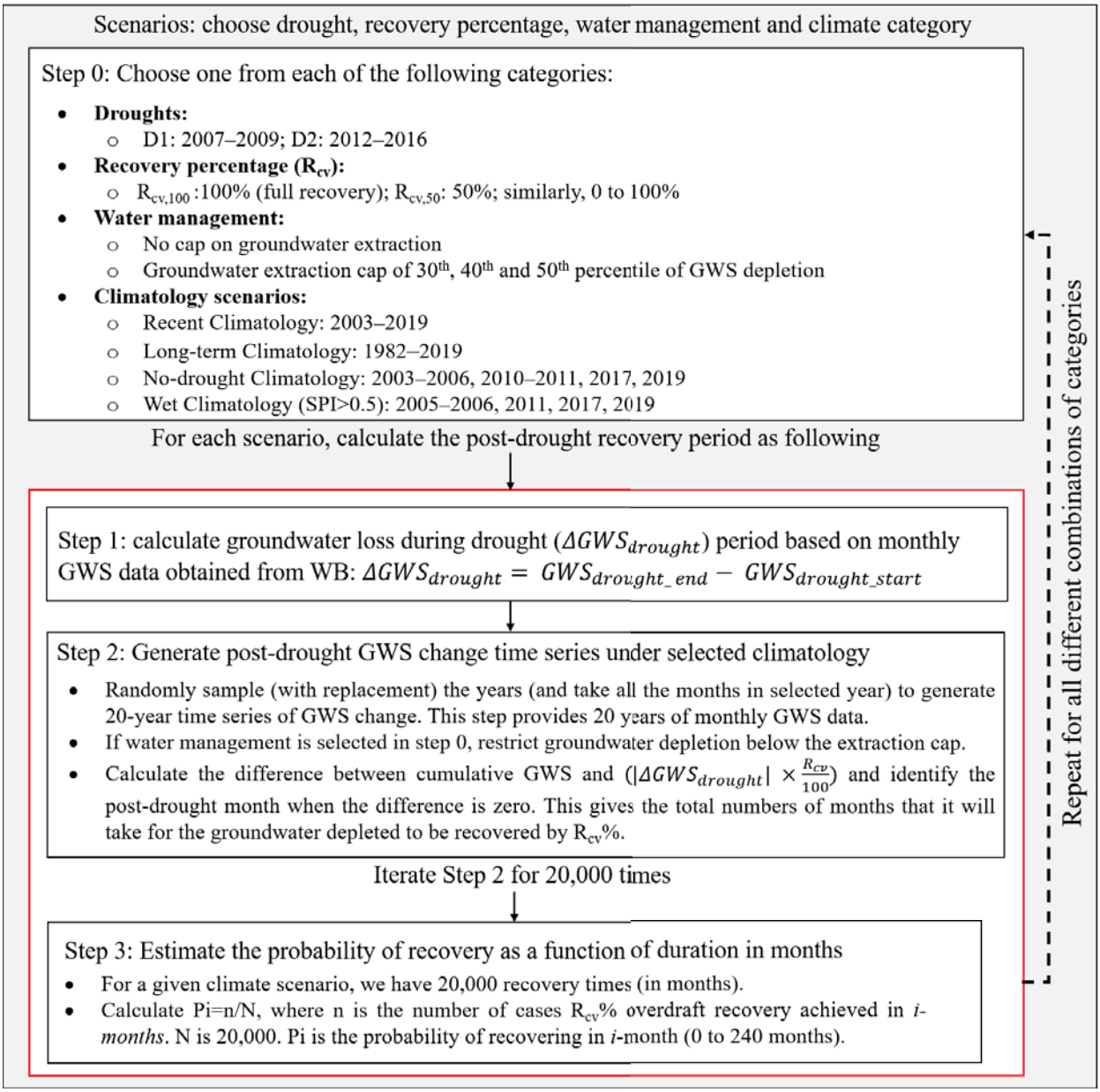

Figure 2. Steps of numerical experiments conducted to estimate post-drought groundwater storage recovery time for two droughts, recovery percentage, two water management options, and four climate scenarios.

In order to consider water management options, we considered the following scenarios:

- No cap on groundwater extraction, which is the current situation in the CV.

- Cap on groundwater extraction, which is likely the future scenario following the implementation of SGMA that regulates groundwater usage. We considered different caps on groundwater extraction: 30th, 40th, and 50th percentile of groundwater depletion rate.

Our numerical experiment approach is detailed in Figure 2.

3.4 Post-drought groundwater recovery under future climate change scenarios

We conducted synthetic experiments to assess the sensitivity of recovery times to water availability (i.e., inflow and precipitation over the CV) and evaporative demand and compare with projected changes under future change scenarios. The base scenario assumes that the inflow (and precipitation) is similar to the monthly median of the years 1982 through 2019. We generated an array of GWS time series for different percentage changes in inflow (and precipitation) and ET, and calculated recovery times for all combinations. This analysis produced a matrix of recovery times that show its sensitivity to inflow and ET. Furthermore, we compare these with projected changes for 20 Global Climate Models and 2 RCP scenarios: modest global emission (RCP4.5) and high global emission (RCP8.5) (Stocker et al., 2014). Similar method for climate change impact assessment has been found effective in earlier studies (Brown et al., 2012; Poff et al., 2016).

4 Results and Discussion

4.1 GWS depletion and recovery assessment in the recent decades

4.1.1 GWS depletion and recovery estimates from different methods

GWS changes estimated by the four methods show similar depletion and recovery patterns during 2002-2019 (Figure 3a and Table 2). All methods indicate lower groundwater storage in 2019 compared to 2003, with relatively mild decline during the first drought (2007–2009) and severe decline during the second drought (2012–2016). However, there are important differences in the magnitude, depletion/recovery rates, and seasonal variations for the different methods. GRACE produce relatively higher seasonal GWS variations, whereas WB and

C2VSIM produce much lower seasonal amplitudes. While the GWS from well data is computed for winter months only to reduce potential errors sourcing from pumping wells. GRACE shows relatively high groundwater storage at the end of the study period (2019). The WB and C2VSIM GWS time series are close to each other (see SI, Figure S7-S12 for WB components and uncertainty). C2VSIM GWS is intermediate between WB, GRACE and Well throughout the period. Compared to April-2003, the GWS in March-2019 changed by -19.1 km^3 (GRACE), -32.4 km^3 (WB), -34.1 km^3 (C2VSIM), and -27.1 km^3 (Well). All methods show close agreement in post-drought recovery period when the uncertainty in GWS estimates is 3.9 km^3 and 1.5 km^3 during 2010–2011 and 2017–2019, whereas the uncertainty in GWS change during drought periods are 2.7 km^3 and 3.9 km^3 for 2007–2009 and 2012–2016 droughts, respectively (Table 2). Uncertainties in GWS estimates can be attributed to the limitation of different GWS estimation methods to represent the groundwater dynamic associated with CV-wide groundwater extraction and land use activities. All methods show a depletion in GWS during the 2007–2009 and 2012–2016 droughts, and GWS recovery during post-drought years 2010–2011 and 2017–2019.

Table 2. GWS changes during drought and post-drought years. Drought periods are Jan-2007 to Dec-2009 and Jan-2012 to Dec-2016. Post-drought periods are Jan-2010 to Dec-2011 (or Pd1) and Jan-2017 to Feb-2019 (or Pd2). Percentage post-drought recoveries for Pd1 and Pd2 are shown in columns $R_{f,Pd1}$ and $R_{f,Pd2}$, respectively.

Methods	2007–2009 [km^3]	2010–2011 [km^3]	Recovery $R_{f,Pd1}$ [%]	2012–2016 [km^3]	2017–2019 [km^3]	Recovery $R_{f,Pd2}$ [%]
GRACE	-18.8	9.2	49.1	-27.5	4.0	14.5
WB	-16.5	3.2	19.3	-23.5	6.8	29.1
C2VSIM	-24.0	11.6	48.4	-33.6	3.5	10.3
Well	-19.5	2.4	12.2	-24.6	2.7	10.9
Median	-19.2	6.2	33.9	-26.1	3.8	12.7
Average	-19.7	6.6	32.3	-27.3	4.3	16.2
St. dev.	2.7	3.9	16.7	3.9	1.5	7.6

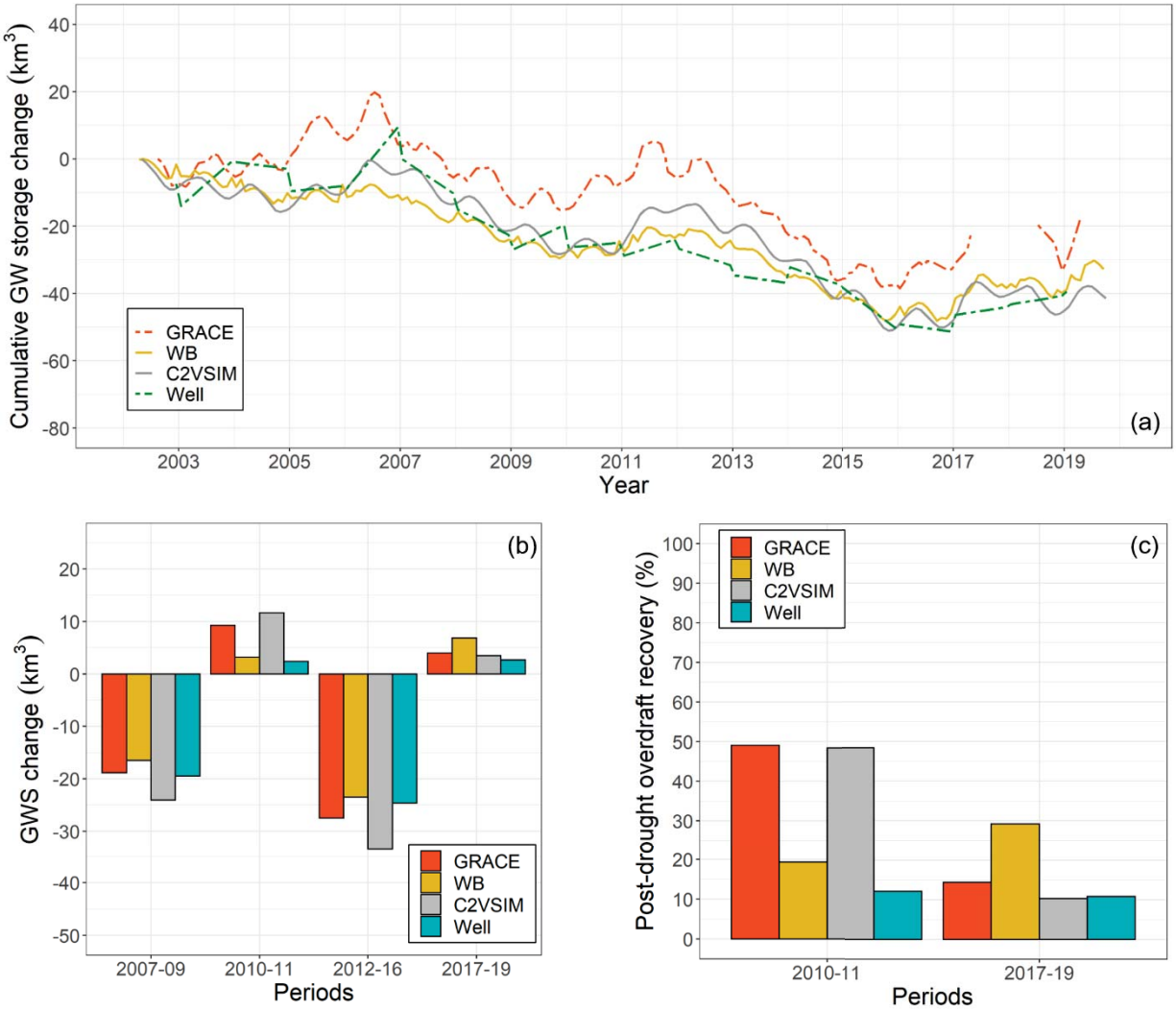

Figure 3. (a) Monthly GWS time series (median estimates) for the CV for April 2002 to September 2019 estimated using the four methods. GRACE GWS is 5-month moving averages to reduce seasonal variability. Well-based GWS is plotted only for winter months: December and January (5-month moving averages), (b) GWS change (km^3) estimates during drought and post-drought years. (c) Percent recovery of GWS from drought during post-drought years.

During the first drought (2007–2009) period, GWS changes from Jan-2007 to Dec-2009 were in the range -24 to -16.5 km^3, depending on the method used, with C2VSIM indicating the greatest depletion (-24 km^3), and the WB indicating the least depletion (-16.5 km^3) (Figure 3b). During the subsequent post-drought period (2010–2011), GWS increased in 2011 compared to 2010 ranged from 2.4 to 11.6 km^3, with C2VSIM indicating the highest recovery (11.6 km^3),

followed by GRACE (9.2 km^3), with WB (3.2 km^3) and Well (2.4 km^3) showing lowest recovery. Comparison of the post-drought (2010–2011) and drought (2007–2009) periods GWS estimates from four methods (in the order Well, WB, CVISIM, and GRACE) showed on median 34% of the GWS depleted during the drought was recovered during the post-drought years (Figure 3c).

In the second and more-severe drought (2012–2016), the GWS changes from to Jan-2012 to Dec-2016 ranged from -23.5 to -33.6 km^3, with GRACE, WB and Well data showing relatively similar changes (-27.5, -23.5, and -24.6 km^3, respectively), while C2VSIM showed relatively higher depletion (-33.6 km^3) (Table 2). High GWS depletion in 2012–2016 is attributed to a longer dry period and greater drought-affected area that strongly increased groundwater dependence (Alam et al., 2019). During the subsequent post-drought years (2017–2019), the GWS increase was low compared to the large overdraft created during the drought of 2012–2016 for all methods. GWS in Feb-2019 increases relative to Jan-2017 ranged from 2.7 to 6.8 km^3, with WB showing largest recovery (6.8 km^3), while GRACE, C2VSIM and Well data indicated similar and small recoveries (4, 3.5, and 2.7 km^3). Overall, the groundwater storage recoveries from the 2012–2016 drought were relatively small (on median 13%). As noted above, post-drought recoveries from the 2007–2009 drought were mostly higher than for the 2012–2016 drought, although all estimates in this case as well were less than 50% of the GWS loss during the prior drought period.

4.1.2 Uncertainties in GWS estimation methods

Despite the variations among the methods, we find the GWS recovery magnitude ranges 2.4–11.6 km^3 during 2010–2011 and 2.7–6.8 km^3 during 2017–2019 (Table 2), which is relatively small compared to drought period GWS changes of -16.5 km^3 to -24 km^3 and -23.5 km^3 and -33.6 km^3 during the 2007–2009 and 2012–2016 droughts. In terms of percentages, the post-drought GWS recovery ranges 12.2–49.1% during 2010–2011 and 10.3–29.1% during 2017–2019. In the previous section, we presented the median GWS changes from each method. Here, we discuss how the uncertainty in different methods affects the GWS estimates.

The GRACE-based GWS estimate in our analysis could be estimated from two different sources of GRACE datasets (JPL-m vs CSR-m). There are differences in GRACE-based GWS

459 estimates between CSR-m and JPL-m. We find that the GWS estimate from JPL-m more closely
460 matches GWS estimates from other methods (both depletion and recovery; Figure S14 and Table
461 S4 of SI), whereas the CSR-m based estimate shows less groundwater depletion than other
462 methods and very high groundwater recovery during 2010–2011 (69.4%). Differences between
463 JPL-m and CSR-m increased after applying the scaling factor provided by JPL intended to
464 reduce signal error (Wiese et al., 2016), whereas no scaling factor is available for CSR-m
465 (scaling factor for JPL-m is shown in Figure S15, SI). Therefore, JPL-m based GWS estimate
466 can be used (after applying scaling factor) to reasonably to represent GWS depletion and
467 recovery in the CV. However, we cannot conclusively state one GRACE MasCon product as the
468 best one based on comparison over only the CV region, especially due to CV's small size, north–
469 south orientation, and location near the coast. Although CSR-m shows relatively lower depletion,
470 we follow a conservative approach and take the average of JPL-m and CSR-m to represent
471 GRACE based GWS estimate. The difference in JPL-m and CSR-m estimates caused the GWS
472 recovery percentage to vary from 38% to 69% during 2010–2011 and from 12% to 16% during
473 2017–2019.

474 The well-based GWS estimation is sensitive to the storage coefficient, interpolation
475 method, and well selection criteria. The CV consists of both semi-confined and confined aquifers
476 where knowledge of the storage coefficient is limited. The storage coefficient is the largest
477 source of uncertainty when estimating GWS change from well data (Scanlon et al., 2012). We
478 compared GWS estimates for three different storage coefficients and settled on an effective
479 storage coefficient (Se = 0.06) (see Text S5 and Figure S16-S8 provides more information on
480 storage coefficient and uncertainty in well-based GWS). The difference in the storage
481 coefficients from multiple sources affect the magnitude of change, while keeping the percentage
482 recovery same (as similar head change used with different storage coefficients). Regarding
483 interpolation, although we used the IDW method, we also tested Kriging and found that the
484 uncertainty associated with the interpolation method is much less than the uncertainty associated
485 with the storage coefficient. We used all types of well data (pumped as well as observation) to
486 generate well-based GWS time series, which means some measurements are affected by the cone
487 of depression from pumping. However, groundwater pumping is typically less during the wet
488 season (November through March) and hence well observations during this period should be

much less affected by pumping. In our calculation of GWS changes during drought and post-drought years, we compared GWS values for months in the wet season only (i.e., December or January, in the interest of omitting "shoulder" months) after taking a 5-month moving average (which captures GWS signal during the entire wet season). Therefore, well-based GWS changes estimated during and after drought years (Figure 3b) should be relatively unaffected by pumping. Furthermore, we computed GWS changes using observation wells, and found that the observation-well based GWS time series does not capture the seasonal pattern. This limited capacity of the observation well data is attributed to significantly lower numbers of measurements compared to the large area of the CV. Different approaches (interpolation methods, varying moving average time window) caused the GWS recovery percentage to vary from 0% to 44% during 2010–2011 and from 4% to 13% during 2017–2019.

The WB-based GWS estimation in CV depends on the storage (i.e., soil moisture, SWE, and reservoir) and flux terms (i.e., inflow, outflow, ET). Average changes in storage term during 2003–2019 is close to zero, and the magnitude of changes are relatively smaller than flux terms. Among the flux terms, we find the inflow to CV has greater uncertainty (standard deviation of 3 km^3/year) than precipitation (standard deviation of 1.42 km^3/year) over the CV. Relatively high uncertainty associated with inflow is intuitive as headwater inflow supply volume is higher than the net precipitation over CV, and multiple sources of inflow data. Since we are using measured outflow, the outflow term does not add uncertainty in our estimation. Difference in WB components caused GWS recovery percentage to vary from around 8% to 69% during 2010–2011 and from 13% to 81% during 2017–2019.

The C2VSIM GWS estimation is affected by uncertain inputs from multiple sources: model parameters (e.g., storage coefficient, hydraulic conductivity, irrigation efficiency), surface water deliveries at different locations, groundwater pumping rates (and location of pumps), and input flux variables (e.g., precipitation, inflow, ET) (CDWR, 2020). In this study, we only used C2VSIM simulations publicly available and have not assessed the uncertainty in overdraft recovery introduced by model inputs and parameters. However, we estimated uncertainty from surface water delivery (relatively low to high surface water allocation) for the 2016-2019 period of C2VSIM simulation that we extended for this study, where we find the GWS recovery percentage during 2017–2019 vary between 2% to 30%.

4.2 GWS recovery assessment under varying climate and water management scenarios

4.2.1 Recovery time under different climatology

We calculated the probability of fully recovering from drought-related groundwater overdraft up to 20-years after drought termination (Figure 4a). The purpose of conducting such an experiment is to understand the response of the aquifer to different climatic conditions and get a sense of the feasibility of recovery from historical groundwater overdraft. The cumulative probability distribution (CDF) of full GWS recovery for the 2007–2009 and 2012–2016 droughts vary significantly for different climatic conditions (i.e., long term climatology, recent climatology, no-drought, and wet years) (Figure 4a). In general, the recovery time for the 2012–2016 drought is longer than that from the 2007–2009 drought, which is attributable to the greater groundwater overdraft during the 2012–2016 drought.

The cumulative distribution of post-drought recovery time shifts significantly from drier (recent climatology) to wetter (wet climatology) conditions, indicating high sensitivity of GWS change to the precipitation and inflow to the CV (Figure 4a). There is less than 10% chance to recover 2007–2009 overdraft in 5 post-drought years under recent climatology, while the chance is much lower for 2012–2016 overdraft (~3%) (Figure 4a). The precipitation and inflow under recent climatology scenario are around 359 ± 26 mm/year and 30 ± 4 km^3/year, respectively. The recent climatology scenario consists of drought events similar to the recent past (2003–2019), therefore drought recovery will be less likely occur as we have already found that the CV GWS has been declining over recent decades (Figure 3a). A similar situation is the case for long-term climatology as the GWS has been declining over past decades due to frequent droughts and increased agricultural water use (Faunt et al., 2009). The recovery time curve for the long-term climatology scenario is close to the recent climatology with relatively longer recovery times (Figure 4a). In the long-term scenario, the existence of longer period droughts (e.g., 1986-1992) in addition to recent droughts results greater recovery times than for any other scenarios (Figure S18 of SI). There is only 15% (or less) chance to fully recover 2007–2009 drought overdrafts in 20 years (much less chance for 2012–2016 drought). In contrast, there is around 95% chance to recover 2007–2009 overdraft in 5-years under wet climatology, which is around 85% for 2012–2016 overdraft. The precipitation and inflow during the wet climatology are around 513 ± 6

548 mm/year and 52 ± 3.5 km^3/year, respectively. Under no-drought climatology, there is around
549 48% chance to recover 2007-2006 overdraft in 5-years (~20% for 2012–2016 overdraft). At a
550 relatively higher probability level (i.e., 80%), it would require 13-18 years to recover from both
551 droughts under the no-drought conditions. Here, the precipitation and inflow during no-drought
552 climate are around 451 ± 17 mm/year and 40 ± 4 km^3/year, respectively. Comparing the recovery
553 times between wet climatology and no-drought climatology, we find that the recovery time for
554 the no-drought climatology is on average 2.3 and 3.5 times the recovery time for wet climatology
555 at for 50% and 80% chances, respectively (Figure 4b-e).

556 The post-drought recovery time increases almost linearly with recovery percentage (0-
557 100%), where the slope increases with the cumulative probability considered (e.g., higher slope
558 for a cumulative probability of 0.99 than 0.5) (Figure 4b-e). The relationship between recovery
559 time and recovery percentage indicates that it is difficult (if not impossible) to recover drought
560 overdraft. Result shows that it would take 6-8 years to fully recovery overdraft under wet
561 climatology, while it is less likely to have 6-8 consecutive wet years in reality. This indicates that
562 the wet climate spells in California cannot fully recover drought caused overdraft under current
563 water management conditions. From the above analysis, we infer that the CV aquifer is not
564 resilient to droughts (less likely to fully recover) and will require appropriate management
565 strategies to establish groundwater sustainability (as mandated by SGMA).

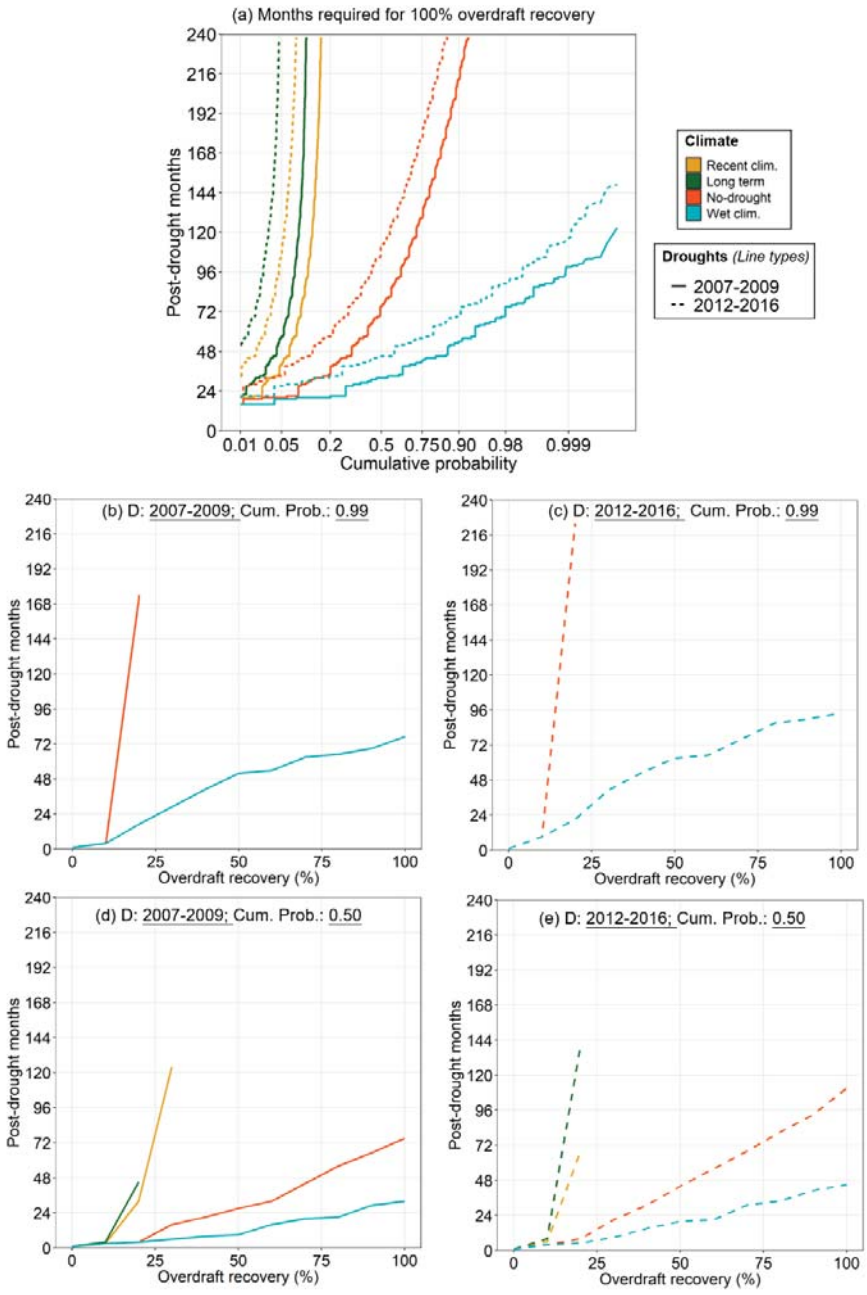

Figure 4. (a) Cumulative probability distribution of months required for 100% recovery of 2007–2009 and 2012–2016 overdrafts. The horizontal axis is plotted on a normal probability scale. (b-e) Months required for varying percentages of overdraft recovery for two droughts (D: 2007–2009 and 2012–2016) and cumulative probabilities (Cum. Prob.: 0.99 and 0.5).

4.2.2 Recovery times for restricted groundwater use scenarios

We calculated overdraft recovery times for scenarios where a groundwater extraction cap is implemented. We analyzed three extraction cap scenarios equal to the 30^{th}, 40^{th} and 50^{th} percentiles of historic GWS depletion. For a given scenario (e.g., 30^{th} percentile restriction), ΔGWS below the threshold is restricted. To estimate the cap magnitude for a given percentile, we first identified negative GWS changes during 2003–2019. Then we estimated the 30^{th}, 40^{th}, and 50^{th} percentiles of these negative GWS changes (Figure S19 of SI). The resultant magnitudes are -1.44 km^3/month, -1.19 km^3/month and -1.02 km^3/month for 30^{th}, 40^{th} and 50^{th} percentile, respectively (below which groundwater depletion is restricted under selected scenarios). Figure 5 shows the cumulative probability distribution of groundwater recovery times for (a) 2007–2009 and (b) 2012–2016 droughts after applying extraction caps. The extraction caps strongly affect the recovery times under the no-drought, recent, and long-term climatology scenarios, whereas they make little difference in the wet climatology scenario. The volume of reduced groundwater extraction under no-drought, recent, and long-term climatology scenarios vary between 2.1-2.6 km^3, 1.5-2.1 km^3, and 1-1.5 km^3/year for 50^{th}, 40^{th}, and 30^{th} percentile groundwater extraction caps, the value of which are 1.9, 1.5, and 1 km^3/year respectively for wet climatology. The limited effects of the caps under wet climatology are attributable to a much lower number of times when ΔGWS goes below the cap, hence the cap is rarely implemented. To demonstrate how effective the extraction cap would be, we extracted recovery times for cumulative probability levels 0.5 (moderate) and 0.8 (high chance) from Figure 5. For these probability levels the recovery times for recent and long-term climatology are beyond maximum time period of the analysis (240 months or 20 years; Figure 4), in other words, there is less than 50% chance to recover in less than 20 years under these scenarios. Therefore, we compared recovery times for no-drought and wet climatology scenarios.

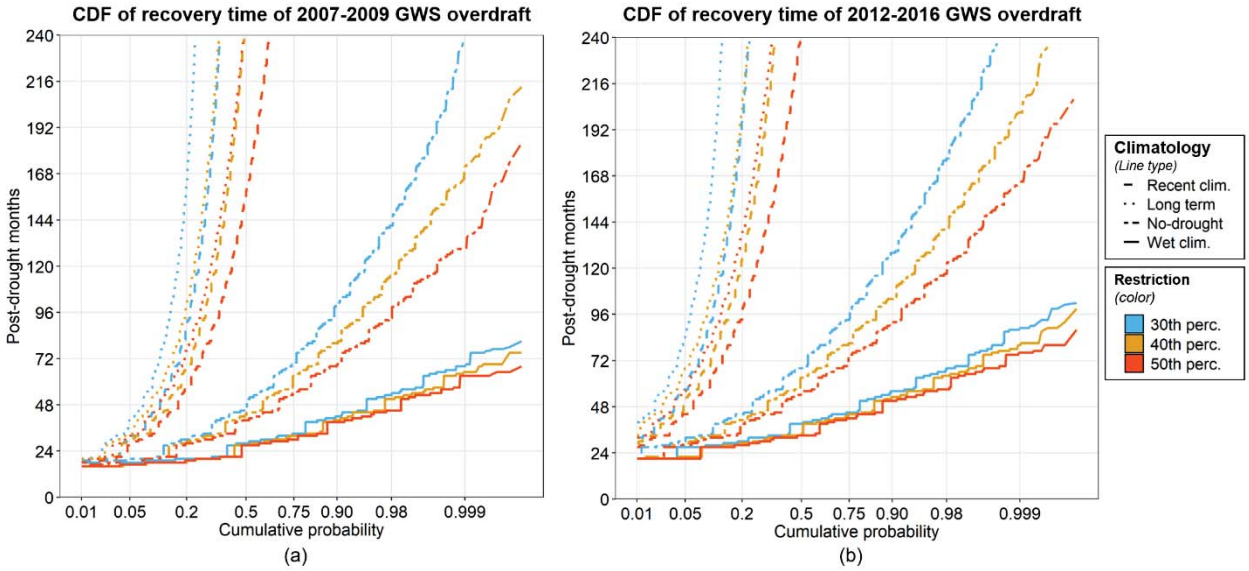

Figure 5. Cumulative distribution of recovery times for groundwater overdraft during (a) 2007–2009 and (b) 2012–2016 droughts. Recovery time is shown after implementation of 30th, 40th, and 50th percentile groundwater extraction caps.

The results show that the groundwater extraction caps significantly reduce the drought-linked GWS recovery time under the no-drought scenario. Groundwater recovery times for full recovery decreases by factors of 1.8 ± 0.1 (3.3± 0.8 years reduced) and 2.3 ± 0.3 (8.1± 1.4 years reduced) after applying an extraction cap for probability levels of 0.5 and 0.8, respectively (see SI, Table S5-S8). The recovery time for the 50th percentile restriction reduces recovery times by 0.4-1 year and 1.8-2.2 years more than for the 30th percentile under 0.5 and 0.8 probability levels, respectively. In contrast, recovery times is reduced by factors of 1.2-1.3 under the wet climatology, which is relatively small as discussed above. Furthermore, recovery times were reduced significantly under recent and long-term climatology. For instance, at a probability level of 0.2 the recovery times (for full recovery) under recent and long-term climatology exceeded 20 years (Figure 4), whereas they were reduced to 5-10 years under the extraction cap (lower recovery time for 50% extraction cap), which is a reduction by a factor of 2-4 times or more. This is due to the greater number of occurrences when GWS depletion goes below the threshold (thereby, extraction cap being implemented). Although our results show that implementation of groundwater extraction caps can improve aquifer resilience to drought, we acknowledge that the impact can vary regionally (south vs north CV), and the actual recovery times can vary. In

particular, the southern CV has greater groundwater overdraft and groundwater dependence than the north. Therefore, the impact of extraction caps on the southern CV is expected to be higher. Moreover, reduction of groundwater extraction implies that there will be less water for irrigation, suggesting a decline in crop production.

4.3 Evaluate the impact of climate change on post-drought recovery time

We evaluated the relative influence of ET and inflow changes on groundwater overdraft recovery time and predicted how the recovery time is expected to change under future climate change. Figure 6 shows the changes in recovery times for different ET and inflow changes. Under historical average condition (average of 1982–2019), 2012–2016 groundwater overdraft was impossible to fully recover as evident from the location of black dot in the unsustainable zone (Figure 6a). However, a marginal increase in average inflow can have a major impact on recovery time when moving from the no-recovery zone to the recovery zone (recovery zone is shown by color shades in Figure 6a). For instance, a 10% increase in average inflow (assuming ET remains the same) will have a recovery time of ~30 years, whereas a 20% increase will have a recovery time of ~9 years (~5 years for 30% increase). However, reducing the recovery time to 1-2 years requires a much greater increase in average inflow. Increases in inflow of around 43% and 60% (compared to the average condition and assuming no ET change) are required for recovery times of 1 and 2 years, respectively. In the past two decades, inflows for almost all years (except years 2010, 2011, 2017, and 2019) were less than the long-term average. While past inflow variability was high (coefficient of variation of annual inflow = 0.32), ET variations were much less (coefficient of variation of annual ET = 0.05).

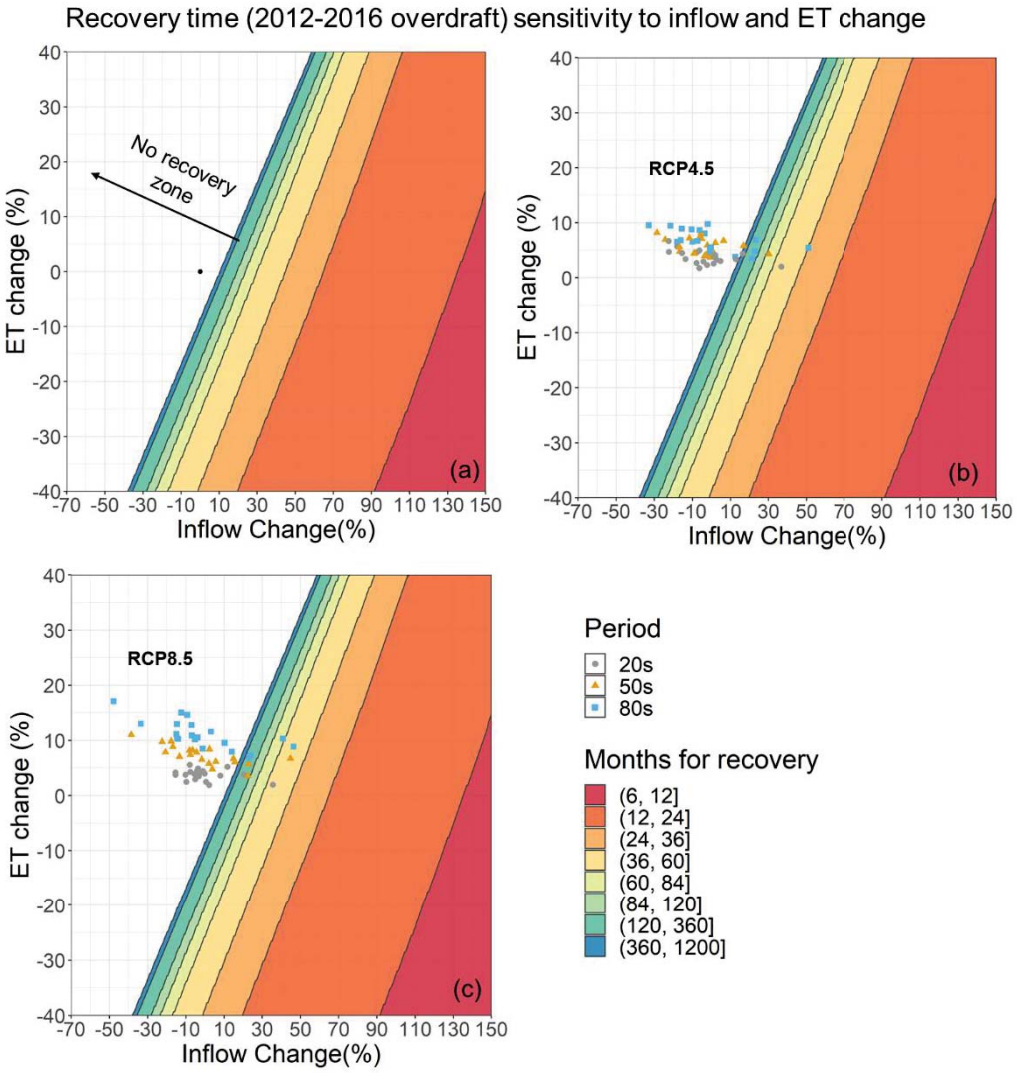

Figure 6. Sensitivity of GWS overdraft (from 2012–2016 drought) recovery time to changes in inflow and ET (a-c). The colors show recovery time bands for different ranges of months. (a) The black dot represents the average historic condition (1982–2019). Projected changes in inflow and ET are shown for (b) RCP4.5 and (c) RCP8.5 scenarios over the sensitivity map (projected changes were obtained from Alam et al. (2019)). The color of the dots (b-c) represents projected changes for three periods 2020s (2010-2039), 2050s (2040-2069), and 2080s (2070-2099).

The projected changes in the recovery time map move further from the average condition into the no-recovery zone, where the negative impact is higher for RCP8.5 (Figure 6c) compared with RCP4.5 (Figure 6b). Overall, it is evident that historical conditions led to chronic groundwater depletion where drought recovery will be difficult to achieve, whereas future

climate will exacerbate the problem manyfold. Therefore, in addition to reducing groundwater use (as shown in section 4.2), increasing recharge of excess water can potentially have important impacts under future climate. Because future climate will change the seasonality of surface water inflow to the CV (increased winter flow and decreased summer flow) (Gergel et al., 2017; Li et al., 2017), more water is expected to leave the CV region during the winter season without being used or stored for later use. Earlier studies show that strategies, such as managed aquifer recharge, can recharge excess surface water (Alam et al., 2021; Gailey et al., 2019; Scanlon et al., 2016; Wendt et al., 2021) and can potentially act as an important adaptation strategy to climate change. The method developed in this study to generate recovery time sensitivity map (Figure 6) can be a useful tool for water managers and planners to estimate post-drought duration required for overdraft recovery. This drought recovery time map is unique from any previous study and can be used to identify potential strategies to minimize the groundwater overdraft recovery times.

5 Summary and conclusions

Groundwater is a critical source of the CV's water supply; however, the resource has been used unsustainably in the past, particularly during droughts, leading to progressive groundwater depletion. Quantifying drought-related groundwater depletion and post-drought recovery and understanding the role of climate and water management in recovering from overdraft is key to establishing a more sustainable management program. We have addressed these issues by quantifying drought-associated groundwater depletion and recovery for two recent droughts (2007–2009 and 2012–2016) using four methods, (GRACE satellite data, water balance approach, the C2VSIM model, and well-measurements). The study reveals the value of considering multiple methods for GWS estimation. Additionally, we used numerical experiments to estimate the probability of post-drought recovery times under different climatic conditions. Based on our analysis, we conclude that:

- Groundwater storage in the CV declined by a median of 19 km^3 (17-24 km^3) and 26 km^3 (24-35 km^3) during the 2007–2009 and 2012–2016 droughts, respectively based on the four methods. The median drought-related overdraft recovery was 34% and 13% during

676 the post-drought years 2010–2011 and 2017–2019, respectively. The relatively low
677 recovery from the 2012–2016 overdraft is attributable to the very large overdraft
678 compared to limited surface water availability during post-drought years. In general,
679 estimates of GWS changes using different methods show similar patterns, but different
680 magnitude. Because there is variability in GWS estimates from different methods that is
681 expected to vary between regions, no one method can be identified as the best. Instead,
682 the multi-method ensemble provides a better overall picture of GWS depletion and post-
683 drought recovery.

684 • Surface water availability (surface inflows to the CV and precipitation) greatly influence
685 the recovery of drought-associated groundwater overdraft. Recovery from drought-
686 related overdrafts is unlikely if the recent climatology (2003–2019) continues after the
687 drought ends (less than 20% chance to fully recover in 20 years). This is because
688 drought-related overdraft in the CV continues and accelerates long-term GWS depletion.
689 Relative to replicated historical climatology, projected drought recovery times decrease
690 by a factor of up to 3.6 for futures with no drought years and by a factor of 7.8 for futures
691 with wet years only. The practical implication is that under current management policies,
692 the CV aquifers are not resilient to drought events — appropriate management measures
693 are needed to establish sustainability.

694 • A cap on groundwater depletion would accelerate groundwater recovery considerably,
695 especially if post-drought conditions are relatively dry. This is because groundwater
696 extraction volume is larger during dry years and tends to exceed any extraction cap more
697 often than for the case of wet climatology when the cap is rarely implemented. Overdraft
698 recovery times decreases by ~2x with implementation of pumping restrictions to
699 constrain groundwater depletion relative to no restrictions under no-drought climatology,
700 with ~2-4x or more if climatology remains at the historical levels. This indicates the
701 important role of reducing groundwater extraction to accelerate overdraft recovery and
702 establish groundwater sustainability.

703 • The CV aquifer is currently managed unsustainably, hence full post-drought recovery is
704 difficult (if not impossible) under the historical average (2003–2019) headwater inflows
705 and crop water use conditions. A marginal increase in average inflow can have a

substantial impact on drought recovery time. An increase in headwater inflow from 10% to 20% (of historic average) would reduce the drought recovery time from 30 years to 9 years. In addition, climate change will make it more challenging to recover from drought-related overdrafts.

Acknowledgements

We thank Hyongki Lee at University of Houston for helpful discussions and advice regarding GRACE MasCon solutions. The University of California Research Initiatives Award LFR-18-548316 supported this work. GRACE CSR RL06 MasCon solutions were obtained from http://www2.csr.utexas.edu/grace and JPL MasCon solutions were obtained from https://podaac-tools.jpl.nasa.gov. The VIC-4.1.2.g code is available at https://doi.org/10.5281/zenodo.4695040. The VIC model parameter and forcing can be obtained from ftp://livnehpublicstorage.colorado.edu/public/ and ftp://livnehpublicstorage.colorado.edu/public/Livneh.2015.NAmer.Dataset/nldas.vic.params/ respectively. Data used in this study are archived at https://doi.org/10.6084/m9.figshare.14544381.v1.

References

Alam, S., Borthakur, A., Ravi, S., Gebremichael, M., Mohanty, S., 2021. Managed aquifer recharge implementation criteria to achieve water sustainability. Sci. Total Environ. 144992. https://doi.org/10.1016/j.scitotenv.2021.144992

Alam, S., Gebremichael, M., Li, R., 2019a. Remote sensing-based assessment of the crop, energy and water nexus in the Central Valley, California. Remote Sens. 11. https://doi.org/10.3390/rs11141701

Alam, S., Gebremichael, M., Li, R., Dozier, J., Lettenmaier, D.P., 2020. Can Managed Aquifer Recharge mitigate the groundwater overdraft in California's Central Valley? Water Resour. Res. e2020WR027244.

Alam, S., Gebremichael, M., Li, R., Dozier, J., Lettenmaier, D.P., 2019b. Climate change impacts on groundwater storage in the Central Valley, California. Clim. Change 157, 387–406.

735 Argus, D.F., Landerer, F.W., Wiese, D.N., Martens, H.R., Fu, Y., Famiglietti, J.S., Thomas, B.F.,
736 Farr, T.G., Moore, A.W., Watkins, M.M., 2017. Sustained Water Loss in California's
737 Mountain Ranges During Severe Drought From 2012 to 2015 Inferred From GPS. J.
738 Geophys. Res. Solid Earth 122, 10,559-10,585. https://doi.org/10.1002/2017JB014424
739 Asoka, A., Gleeson, T., Wada, Y., Mishra, V., 2017. Relative contribution of monsoon
740 precipitation and pumping to changes in groundwater storage in India. Nat. Geosci. 10,
741 109–117.
742 Bettadpur, S., 2012. UTCSR level-2 processing standards document for level-2 product release
743 0005. GRACE Rep 327, 742–742.
744 Brown, C., Ghile, Y., Laverty, M., Li, K., 2012. Decision scaling: Linking bottom-up
745 vulnerability analysis with climate projections in the water sector. Water Resour. Res. 48.
746 Brush, C.F., 2013. Historical Rim Inflows, Surface Water Diversions and Bypass Flows for the
747 California Central Valley Groundwater-Surface Water Simulation Model (C2VSim),
748 Version 3.02-CG. Bay-Delta Office, California Department of Water Resources.
749 California State Legislature, 2014. Sustainable groundwater management act.
750 https://www.opr.ca.gov/docs/2014_Sustainable_Groundwater_Management_
751 Legislation_092914.pdf.
752 CASGEM, 2021. Periodic Groundwater level Measurements. Department of Water Resources
753 California Statewide Groundwater Elevation Monitoring [Data file]. Retrieved from:
754 https://data.cnra.ca.gov/dataset/periodic-groundwater-level-measurements.
755 CDEC, 2020. California Data Exchange Center - Reservoirs. Source:
756 https://cdec.water.ca.gov/reservoir.html.
757 CDWR, 2020. C2VSimFG Version 1.0: Fine Grid California Central Valley Groundwater-
758 Surface Water Simulation Model. Model last updated on December 8, 2020. Available at
759 https://data.cnra.ca.gov/dataset/c2vsimfg-version-1-0.
760 CDWR, 2014. California State Water Project Overview California Dept. Water resources.
761 CDWR, 2013. California Department of Water Resources and California Natural Resources
762 Agency, and State of California. California's groundwater update 2013, A Compilation of
763 Enhanced Content for California (California: Department of Water Resources).

764 Cooper, M.G., Schaperow, J.R., Cooley, S.W., Alam, S., Smith, L.C., Lettenmaier, D.P., 2018.
765 Climate Elasticity of Low Flows in the Maritime Western U.S. Mountains. Water Resour.
766 Res. 54. https://doi.org/10.1029/2018WR022816
767 Daly, C., Halbleib, M., Smith, J.I., Gibson, W.P., Doggett, M.K., Taylor, G.H., Curtis, J.,
768 Pasteris, P.P., 2008. Physiographically sensitive mapping of climatological temperature
769 and precipitation across the conterminous United States. Int. J. Climatol. J. R. Meteorol.
770 Soc. 28, 2031–2064.
771 Dayflow, 2020. Delta boundary hydrology available through California Natural Resources
772 Agency. source: https://data.cnra.ca.gov/dataset/dayflow.
773 DeChant, C.M., Moradkhani, H., 2015. Analyzing the sensitivity of drought recovery forecasts to
774 land surface initial conditions. J. Hydrol. 526, 89–100.
775 Dogrul, E.C., Kadir, T.N., Brush, C.F., 2015. DWR Technical Memorandum and User ' s
776 Manual.
777 Dogrul, E.C., Kadir, T.N., Brush, C.F., Chung, F.I., 2016. Environmental Modelling & Software
778 Linking groundwater simulation and reservoir system analysis models : The case for
779 California ' s Central Valley. Environ. Model. Softw. 77, 168–182.
780 https://doi.org/10.1016/j.envsoft.2015.12.006
781 Famiglietti, J.S., 2014. The global groundwater crisis. Nat. Clim. Change 4, 945–948.
782 Famiglietti, J.S., Lo, M., Ho, S.L., Bethune, J., Anderson, K.J., Syed, T.H., Swenson, S.C., De
783 Linage, C.R., Rodell, M., 2011. Satellites measure recent rates of groundwater depletion
784 in California's Central Valley. Geophys. Res. Lett. 38, 2–5.
785 https://doi.org/10.1029/2010GL046442
786 Farrar, C.D., Bertoldi, G.L., 1988. Region 4, central valley and pacific coast ranges. Hydrogeol.
787 Geol. Soc. N. Am. Boulder Colo. 1988 P 59-67 4 Fig 28 Ref.
788 Faunt, C.C., Hanson, R.T., Belitz, K., Schmid, W., Predmore, S.P., Rewis, D.L., McPherson, K.,
789 2009. Groundwater Availability of the Central Valley Aquifer, California, US.
790 Geological Survey Professional Paper 1766.
791 Faunt, C.C., Sneed, M., Traum, J., Brandt, J.T., 2016. Water availability and land subsidence in
792 the Central Valley, California, USA. Hydrogeol. J. 24, 675–684.

793 Feng, W., Shum, C.K., Zhong, M., Pan, Y., 2018. Groundwater storage changes in China from
794 satellite gravity: An overview. Remote Sens. 10, 674–674.
795 Feng, W., Zhong, M., Lemoine, J., Biancale, R., Hsu, H., Xia, J., 2013. Evaluation of
796 groundwater depletion in North China using the Gravity Recovery and Climate
797 Experiment (GRACE) data and ground-based measurements. Water Resour. Res. 49,
798 2110–2118.
799 Fleming, S.W., Quilty, E.J., 2006. Aquifer responses to el Niño–Southern oscillation, southwest
800 British Columbia. Groundwater 44, 595–599.
801 Gailey, R.M., Fogg, G.E., Lund, J.R., Medellín-Azuara, J., 2019. Maximizing on-farm
802 groundwater recharge with surface reservoir releases: a planning approach and case study
803 in California, USA. Hydrogeol. J. 27, 1183–1206.
804 Gebremichael, M., Krishnamurthy, P.K., Ghebremichael, L.T., Alam, S., 2021. What Drives
805 Crop Land Use Change during Multi-Year Droughts in California's Central Valley?
806 Prices or Concern for Water? Remote Sens. 13, 650–650.
807 Gergel, D.R., Nijssen, B., Abatzoglou, J.T., Lettenmaier, D.P., Stumbaugh, M.R., 2017. Effects
808 of climate change on snowpack and fire potential in the western USA. Clim. Change 141,
809 287–299.
810 Ghasemizade, M., Asante, K.O., Petersen, C., Kocis, T., Dahlke, H.E., Harter, T., 2019. An
811 integrated approach toward sustainability via groundwater banking in the southern
812 Central Valley, California. Water Resour. Res. 55, 2742–2759.
813 Gleeson, T., Wada, Y., Bierkens, M.F.P., Van Beek, L.P.H., 2012. Water balance of global
814 aquifers revealed by groundwater footprint. Nature 488, 197–200.
815 https://doi.org/10.1038/nature11295
816 Hanak, E., 2011. Managing California's water: from conflict to reconciliation. Public Policy
817 Instit. of CA.
818 Hanak, E., Lund, J., Arnold, B., Escriva-Bou, A., Gray, B., Green, S., Harter, T., Howitt, R.,
819 MacEwan, D., Medellín-Azuara, J., 2017. Water stress and a changing San Joaquin
820 Valley. Public Policy Inst. Calif. 1, 5–48.
821 Hanson, R.T., Flint, L.E., Flint, A.L., Dettinger, M.D., Faunt, C.C., Cayan, D., Schmid, W.,
822 2012. A method for physically based model analysis of conjunctive use in response to

potential climate changes. Water Resour. Res. 48, 1–23. https://doi.org/10.1029/2011WR010774

Kourakos, G., Dahlke, H.E., Harter, T., 2019. Increasing groundwater availability and seasonal base flow through agricultural managed aquifer recharge in an irrigated basin. Water Resour. Res. 55, 7464–7492.

Kuss, A.J.M., Gurdak, J.J., 2014. Groundwater level response in US principal aquifers to ENSO, NAO, PDO, and AMO. J. Hydrol. 519, 1939–1952.

Li, D., Wrzesien, M.L., Durand, M., Adam, J., Lettenmaier, D.P., 2017. How much runoff originates as snow in the western United States, and how will that change in the future? Geophys. Res. Lett. 44, 6163–6172.

Livneh, B., Rosenberg, E.A., Lin, C., Nijssen, B., Mishra, V., Andreadis, K.M., Maurer, E.P., Lettenmaier, D.P., 2013. A long-term hydrologically based dataset of land surface fluxes and states for the conterminous United States: Update and extensions. J. Clim. 26, 9384–9392.

Long, D., Chen, X., Scanlon, B.R., Wada, Y., Hong, Y., Singh, V.P., Chen, Y., Wang, C., Han, Z., Yang, W., 2016. Have GRACE satellites overestimated groundwater depletion in the Northwest India Aquifer? Sci. Rep. 6, 24398–24398.

Longuevergne, L., Florsch, N., Elsass, P., 2007. Extracting coherent regional information from local measurements with Karhunen-Loève transform: Case study of an alluvial aquifer (Rhine valley, France and Germany). Water Resour. Res. 43.

Miller, N.L., Dale, L.L., Brush, C.F., Vicuna, S.D., Kadir, T.N., Dogrul, E.C., Chung, F.I., Norman, L., Dale, L.L., Brush, C.F., Vicuna, S.D., Kadir, T.N., Dogrul, E.C., 2009. Drought Resilience of the California Central Valley Surface-Groundwater-Conceyabce System 45. https://doi.org/10.1111/j.1752-1688.2009.00329.x

Ojha, C., Werth, S., Shirzaei, M., 2020. Recovery of aquifer-systems in Southwest US following 2012-2015 drought: evidence from InSAR, GRACE and groundwater level data. J. Hydrol. 124943–124943.

Ojha, C., Werth, S., Shirzaei, M., 2019. Groundwater loss and aquifer system compaction in San Joaquin Valley during 2012–2015 drought. J. Geophys. Res. Solid Earth 124, 3127–3143.

852 Pan, M., Yuan, X., Wood, E.F., 2013. A probabilistic framework for assessing drought recovery.
853 Geophys. Res. Lett. 40, 3637–3642. https://doi.org/10.1002/grl.50728
854 Perez-Valdivia, C., Sauchyn, D., Vanstone, J., 2012. Groundwater levels and teleconnection
855 patterns in the Canadian Prairies. Water Resour. Res. 48.
856 Planert, M., Williams, J.S., 1995. Groundwater atlas of the United States, California, Nevada.
857 HA 730-B. US Geol. Surv. Rest. VA.
858 Poff, N.L., Brown, C.M., Grantham, T.E., Matthews, J.H., Palmer, M.A., Spence, C.M., Wilby,
859 R.L., Haasnoot, M., Mendoza, G.F., Dominique, K.C., 2016. Sustainable water
860 management under future uncertainty with eco-engineering decision scaling. Nat. Clim.
861 Change 6, 25–34.
862 Ralph, F.M., Dettinger, M.D., 2012. Historical and national perspectives on extreme West Coast
863 precipitation associated with atmospheric rivers during December 2010. Bull. Am.
864 Meteorol. Soc. 93, 783–790.
865 Rateb, A., Scanlon, B.R., Pool, D.R., Sun, A., Zhang, Z., Chen, J., Clark, B., Faunt, C.C., Haugh,
866 C.J., Hill, M., 2020. Comparison of Groundwater Storage Changes From GRACE
867 Satellites With Monitoring and Modeling of Major US Aquifers. Water Resour. Res. 56,
868 e2020WR027556-e2020WR027556.
869 Rodell, M., Famiglietti, J.S., 2002. The potential for satellite-based monitoring of groundwater
870 storage changes using GRACE: the High Plains aquifer, Central US. J. Hydrol. 263, 245–
871 256.
872 Russo, T.A., Lall, U., 2017. Depletion and response of deep groundwater to climate-induced
873 pumping variability. Nat. Geosci. 10, 105–108. https://doi.org/10.1038/ngeo2883
874 Save, 2020. CSR GRACE and GRACE-FO RL06 Mascon Solutions v02, doi: 10.15781/cgq9-
875 nh24.
876 Save, H., Bettadpur, S., Tapley, B.D., 2016. High-resolution CSR GRACE RL05 mascons. J.
877 Geophys. Res. Solid Earth 121, 7547–7569.
878 Scanlon, B. R., Faunt, C.C., Longuevergne, L., Reedy, R.C., Alley, W.M., McGuire, V.L.,
879 McMahon, P.B., 2012. Groundwater depletion and sustainability of irrigation in the US
880 High Plains and Central Valley. Proc. Natl. Acad. Sci. 109, 9320–9325.
881 https://doi.org/10.1073/pnas.1200311109

882 Scanlon, Bridget R, Longuevergne, L., Long, D., 2012. Ground referencing GRACE satellite
883 estimates of groundwater storage changes in the California Central Valley, USA. Water
884 Resour. Res. 48.
885 Scanlon, Bridget R., Reedy, R.C., Faunt, C.C., Pool, D., Uhlman, K., 2016. Enhancing drought
886 resilience with conjunctive use and managed aquifer recharge in California and Arizona.
887 Environ. Res. Lett. 11, 035013.
888 Scanlon, Bridget R, Zhang, Z., Save, H., Wiese, D.N., Landerer, F.W., Long, D., Longuevergne,
889 L., Chen, J., 2016. Global evaluation of new GRACE mascon products for hydrologic
890 applications. Water Resour. Res. 52, 9412–9429.
891 Stocker, T.F., Qin, D., Plattner, G.-K., Tignor, M.M.B., Allen, S.K., Boschung, J., Nauels, A.,
892 Xia, Y., Bex, V., Midgley, P.M., 2014. Climate Change 2013: The physical science basis.
893 contribution of working group I to the fifth assessment report of IPCC the
894 intergovernmental panel on climate change.
895 Taylor, R.G., Scanlon, B., Döll, P., Rodell, M., Van Beek, R., Wada, Y., Longuevergne, L.,
896 Leblanc, M., Famiglietti, J.S., Edmunds, M., Konikow, L., Green, T.R., Chen, J.,
897 Taniguchi, M., Bierkens, M.F.P., Macdonald, A., Fan, Y., Maxwell, R.M., Yechieli, Y.,
898 Gurdak, J.J., Allen, D.M., Shamsudduha, M., Hiscock, K., Yeh, P.J.F., Holman, I.,
899 Treidel, H., 2013. Ground water and climate change. Nat. Clim. Change 3, 322–329.
900 https://doi.org/10.1038/nclimate1744
901 Thomas, B.F., Famiglietti, J.S., 2019. Identifying Climate-Induced Groundwater Depletion in
902 GRACE Observations. Sci. Rep. 9, 4124–4124. https://doi.org/10.1038/s41598-019-
903 40155-y
904 Thomas, B.F., Famiglietti, J.S., Landerer, F.W., Wiese, D.N., Molotch, N.P., Argus, D.F., 2017.
905 GRACE groundwater drought index: Evaluation of California Central Valley
906 groundwater drought. Remote Sens. Environ. 198, 384–392.
907 Thornton, P., Thornton, M.M., Mayer, B.M., Wei, Y., Devarakonda, R.S., Vose, R.S., Cook,
908 R.B., 2017. Daymet: Daily Surface Weather Data on a 1-km Grid for North America,
909 Version 3 ORNL DAAC Oak Ridge Tenn.
910 USBR, 2014. Central Valley Project U.S. Department of Interior Bureau of Reclamation.

USDA-NASS, 2020. National Agricultural Statistics Service Cropland Data Layer, Published crop-specific data layer. Available at https://nassgeodata.gmu.edu/CropScape/. USDA-NASS, Washington, DC.

USGS, 2020. National Water Information System data available on the World Wide Web (USGS Water Data for the Nation). source: http://waterdata.usgs.gov/nwis/.

Voss, K., Swenson, S., Rodell, M., Richey, A.S., Thomas, B.F., Lo, M.-H., Reager, J.T., Famiglietti, J.S., 2015. Quantifying renewable groundwater stress with GRACE. Water Resour. Res. 51, 1–22. https://doi.org/10.1002/2015WR017349.Received

Wada, Y., Van Beek, L.P.H., Van Kempen, C.M., Reckman, J.W.T.M., Vasak, S., Bierkens, M.F.P., 2010. Global depletion of groundwater resources. Geophys. Res. Lett. 37, 1–5. https://doi.org/10.1029/2010GL044571

Wahr, J., Molenaar, M., Bryan, F., 1998. Time variability of the Earth's gravity field: Hydrological and oceanic effects and their possible detection using GRACE. J. Geophys. Res. Solid Earth 103, 30205–30229.

Watkins, M.M., Wiese, D.N., Yuan, D., Boening, C., Landerer, F.W., 2015. Improved methods for observing Earth's time variable mass distribution with GRACE using spherical cap mascons. J. Geophys. Res. Solid Earth 120, 2648–2671.

Wendt, D.E., Van Loon, A.F., Scanlon, B.R., Hannah, D.M., 2021. Managed aquifer recharge as a drought mitigation strategy in heavily-stressed aquifers. Environ. Res. Lett. 16, 14046–14046.

Wiese, D.N., Landerer, F.W., Watkins, M.M., 2016. Quantifying and reducing leakage errors in the JPL RL05M GRACE mascon solution. Water Resour. Res. 52, 7490–7502.

Wu, W.-Y., Lo, M.-H., Wada, Y., Famiglietti, J.S., Reager, J.T., Yeh, P.J.-F., Ducharne, A., Yang, Z.-L., 2020. Divergent effects of climate change on future groundwater availability in key mid-latitude aquifers. Nat. Commun. 11, 1–9.

Xiao, M., Koppa, A., Mekonnen, Z., Pagán, B.R., Zhan, S., Cao, Q., Aierken, A., Lee, H., Lettenmaier, D.P., 2017. How much groundwater did California's Central Valley lose during the 2012–2016 drought? Geophys. Res. Lett. 44, 4872–4879.

Figure 1.

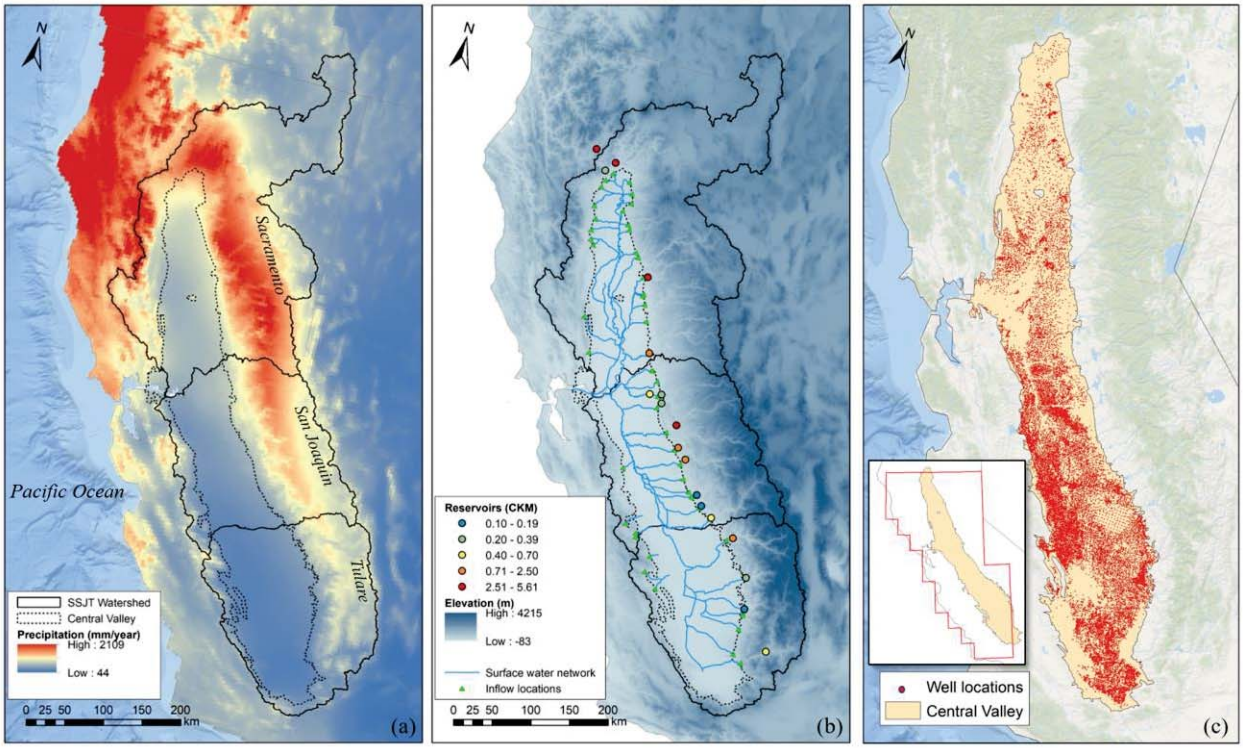
N
Sacramento
San Joaquin
Tulare
Pacific Ocean
SSJT Watershed
Central Valley
Precipitation (mm/year)
High : 2109
Low : 44
0 25 50 100 150 200
km
(a)
N
Reservoirs (CKM)
0.10 - 0.19
0.20 - 0.39
0.40 - 0.70
0.71 - 2.50
2.51 - 5.61
Elevation (m)
High : 4215
Low : -83
Surface water network
Inflow locations
0 25 50 100 150 200
km
(b)
N
Well locations
Central Valley
(c)

Figure 2.

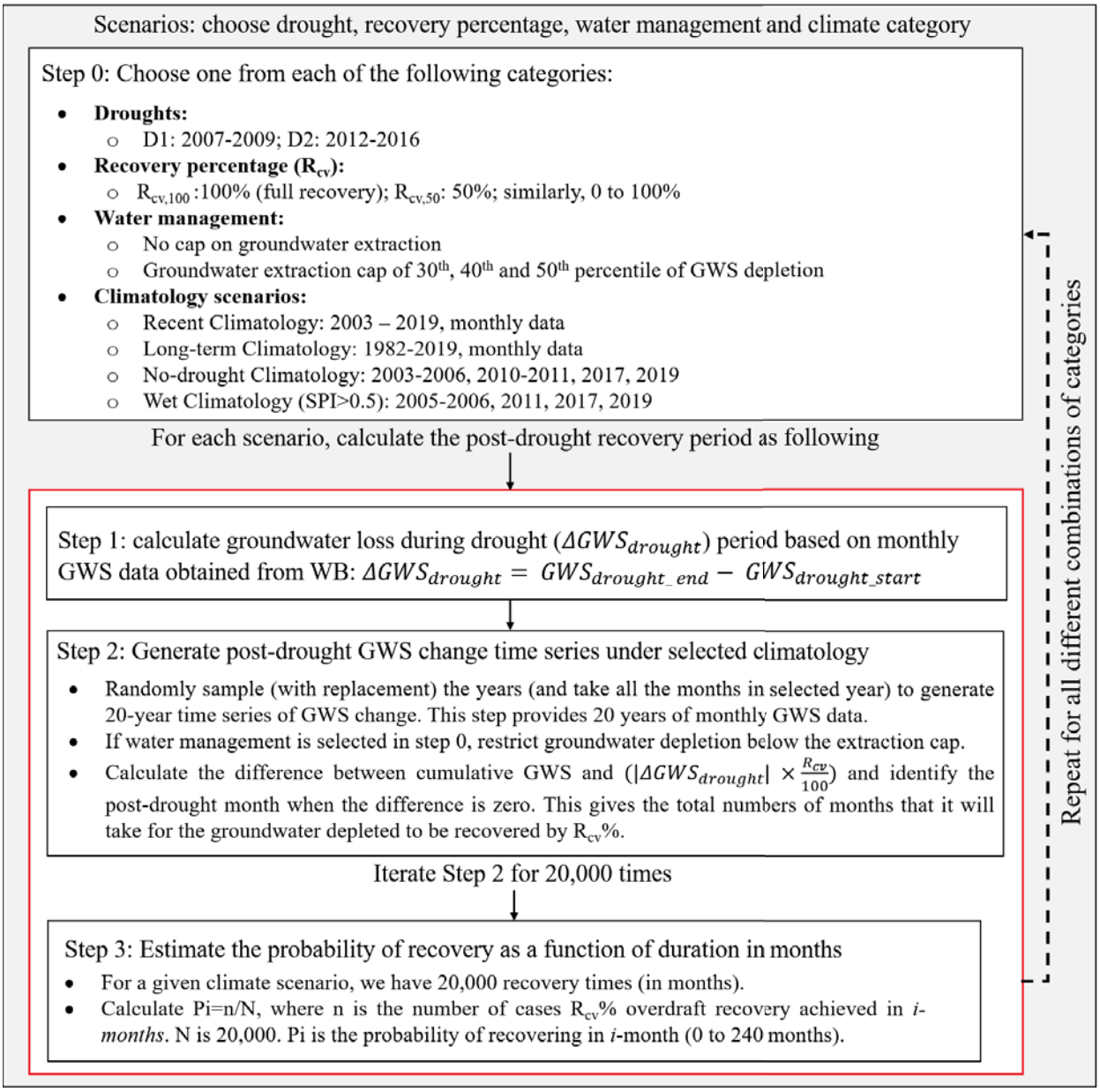
Scenarios: choose drought, recovery percentage, water management and climate category
Step 0: Choose one from each of the following categories:
Droughts:
D1: 2007-2009; D2: 2012-2016
Recovery percentage (R_{cv}):
$R_{cv,100}$:100% (full recovery); $R_{cv,50}$: 50%; similarly, 0 to 100%
Water management:
No cap on groundwater extraction
Groundwater extraction cap of 30th, 40th and 50th percentile of GWS depletion
Climatology scenarios:
Recent Climatology: 2003 – 2019, monthly data
Long-term Climatology: 1982-2019, monthly data
No-drought Climatology: 2003-2006, 2010-2011, 2017, 2019
Wet Climatology (SPI>0.5): 2005-2006, 2011, 2017, 2019
For each scenario, calculate the post-drought recovery period as following
Step 1: calculate groundwater loss during drought ($\Delta GWS_{drought}$) period based on monthly GWS data obtained from WB: $\Delta GWS_{drought} = GWS_{drought\_end} - GWS_{drought\_start}$
Step 2: Generate post-drought GWS change time series under selected climatology
Randomly sample (with replacement) the years (and take all the months in selected year) to generate 20-year time series of GWS change. This step provides 20 years of monthly GWS data.
If water management is selected in step 0, restrict groundwater depletion below the extraction cap.
Calculate the difference between cumulative GWS and ($|\Delta GWS_{drought}| \times \frac{R_{cv}}{100}$) and identify the post-drought month when the difference is zero. This gives the total numbers of months that it will take for the groundwater depleted to be recovered by R_{cv}%.
Iterate Step 2 for 20,000 times
Step 3: Estimate the probability of recovery as a function of duration in months
For a given climate scenario, we have 20,000 recovery times (in months).
Calculate Pi=n/N, where n is the number of cases R_{cv}% overdraft recovery achieved in i-months. N is 20,000. Pi is the probability of recovering in i-month (0 to 240 months).
Repeat for all different combinations of categories

Figure 3.

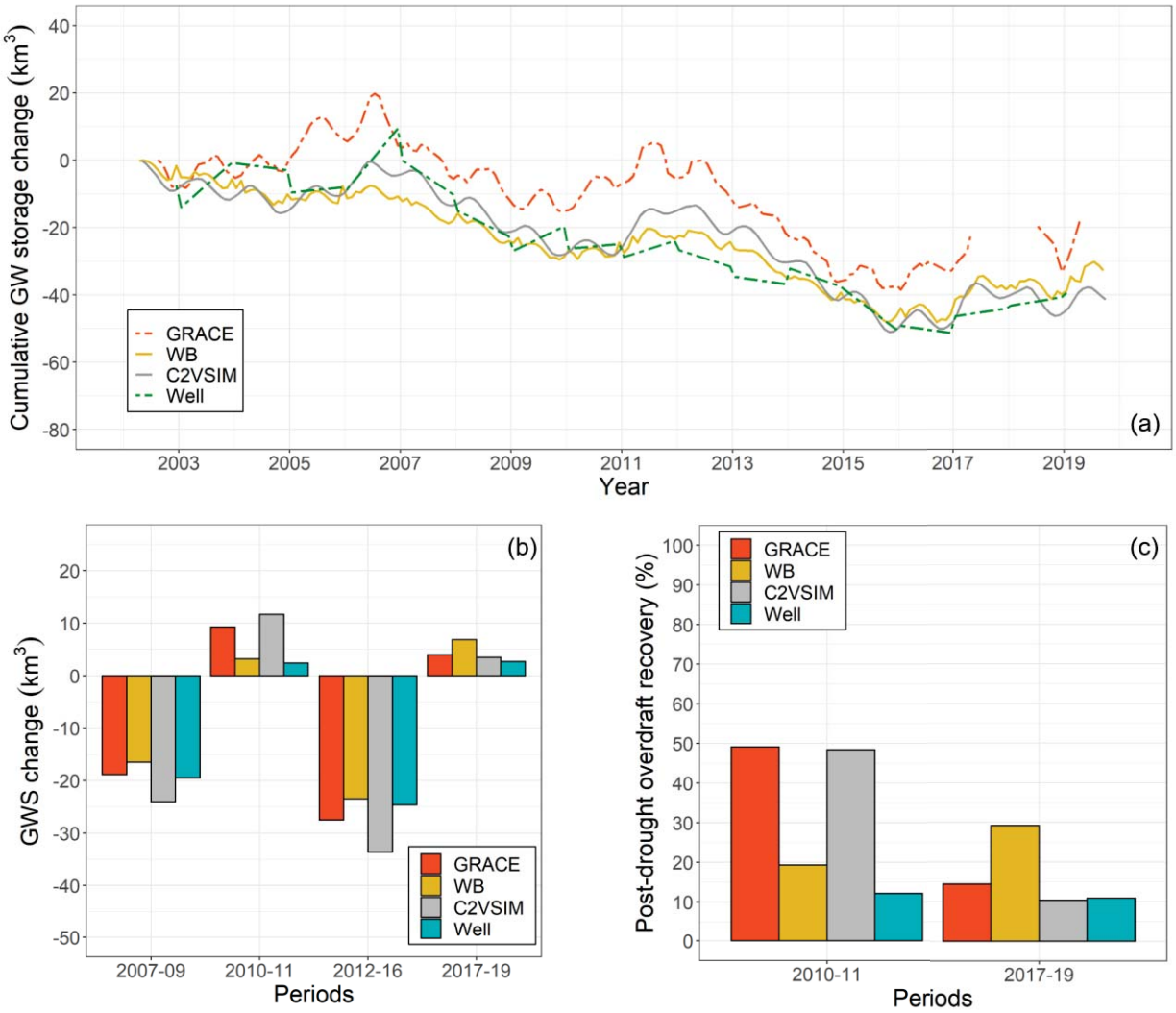
Cumulative GW storage change (km3)
40
20
0
-20
-40
-60
-80
GRACE
WB
C2VSIM
Well
(a)
2003
2005
2007
2009
2011
2013
2015
2017
2019
Year
GWS change (km3)
20
10
0
-10
-20
-30
-40
-50
(b)
GRACE
WB
C2VSIM
Well
2007-09
2010-11
2012-16
2017-19
Periods
Post-drought overdraft recovery (%)
100
90
80
70
60
50
40
30
20
10
0
(c)
GRACE
WB
C2VSIM
Well
2010-11
2017-19
Periods

Figure 4.

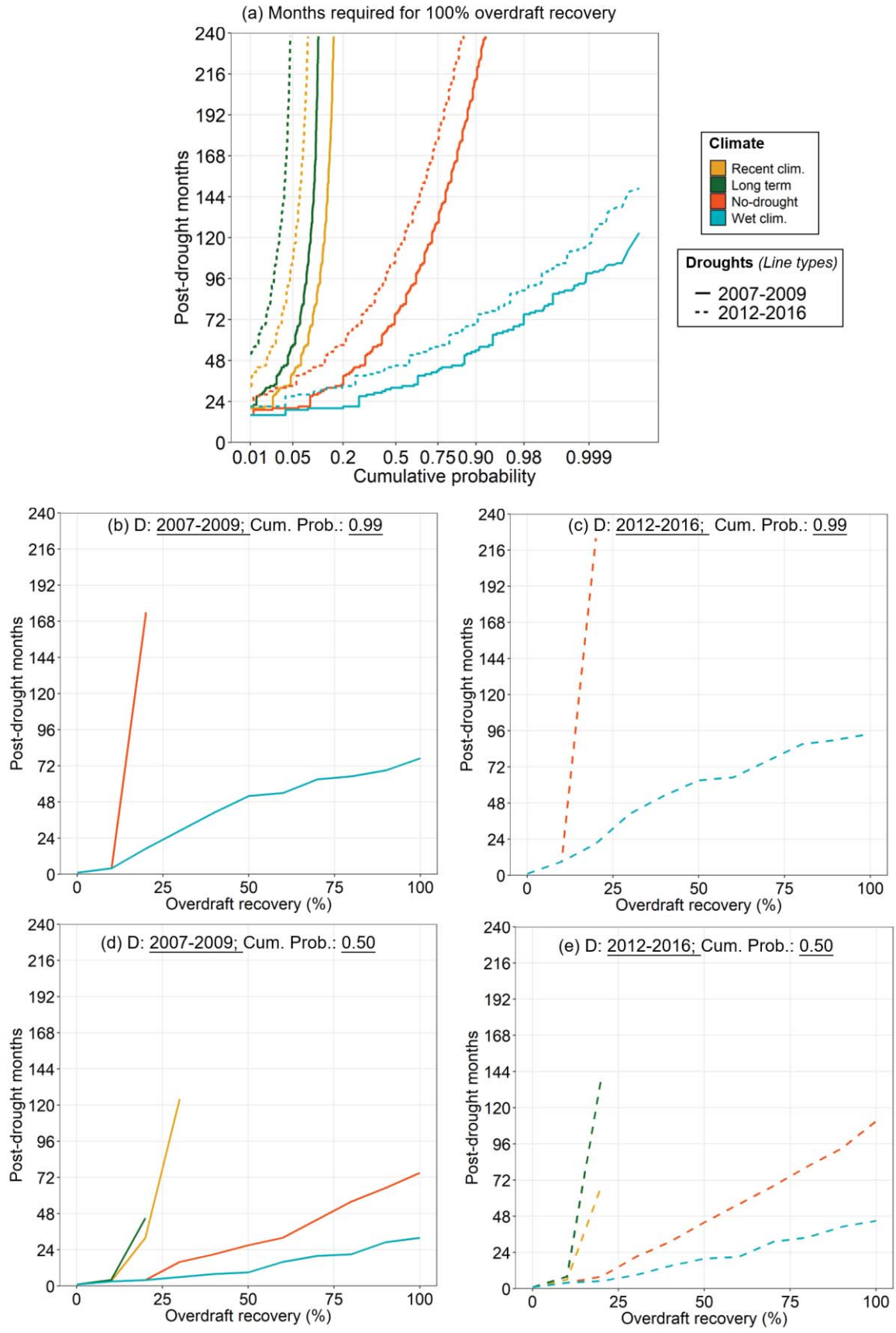
(a) Months required for 100% overdraft recovery
Post-drought months
Cumulative probability
0.01 0.05 0.2 0.5 0.75 0.90 0.98 0.999
Climate
Recent clim.
Long term
No-drought
Wet clim.
Droughts (Line types)
2007-2009
2012-2016
(b) D: 2007-2009; Cum. Prob.: 0.99
(c) D: 2012-2016; Cum. Prob.: 0.99
(d) D: 2007-2009; Cum. Prob.: 0.50
(e) D: 2012-2016; Cum. Prob.: 0.50
Overdraft recovery (%)

Figure 5.

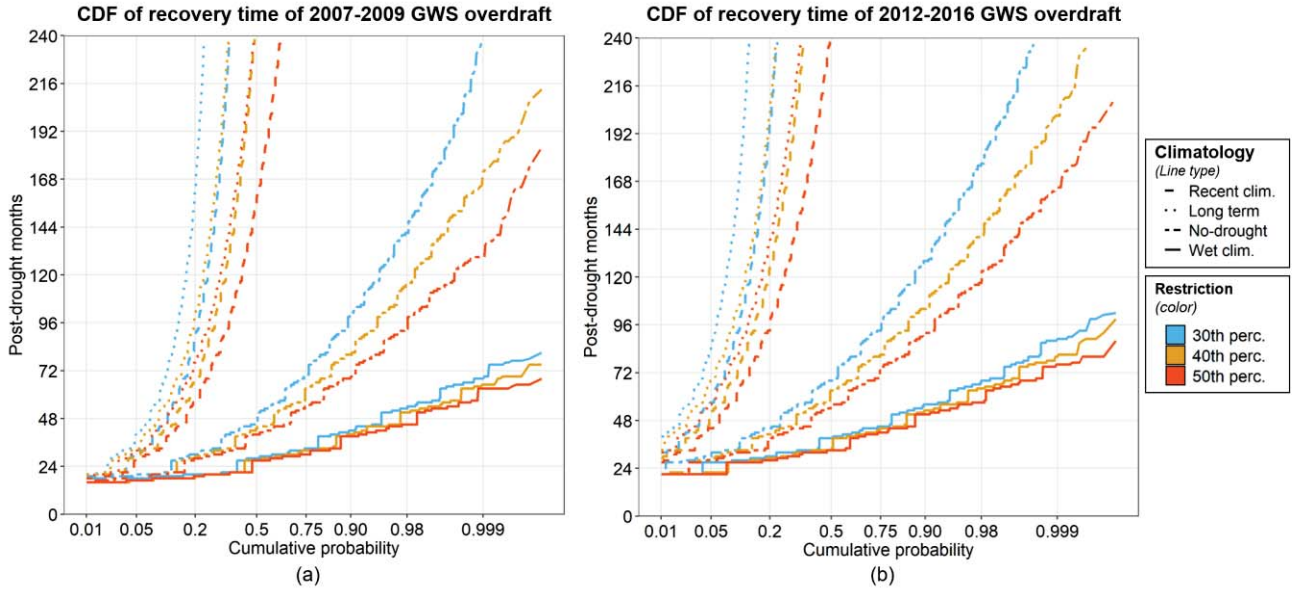
CDF of recovery time of 2007-2009 GWS overdraft
CDF of recovery time of 2012-2016 GWS overdraft
Post-drought months
0
24
48
72
96
120
144
168
192
216
240
0.01
0.05
0.2
0.5
0.75
0.90
0.98
0.999
Cumulative probability
(a)
(b)
Climatology
(Line type)
Recent clim.
Long term
No-drought
Wet clim.
Restriction
(color)
30th perc.
40th perc.
50th perc.

Figure 6.

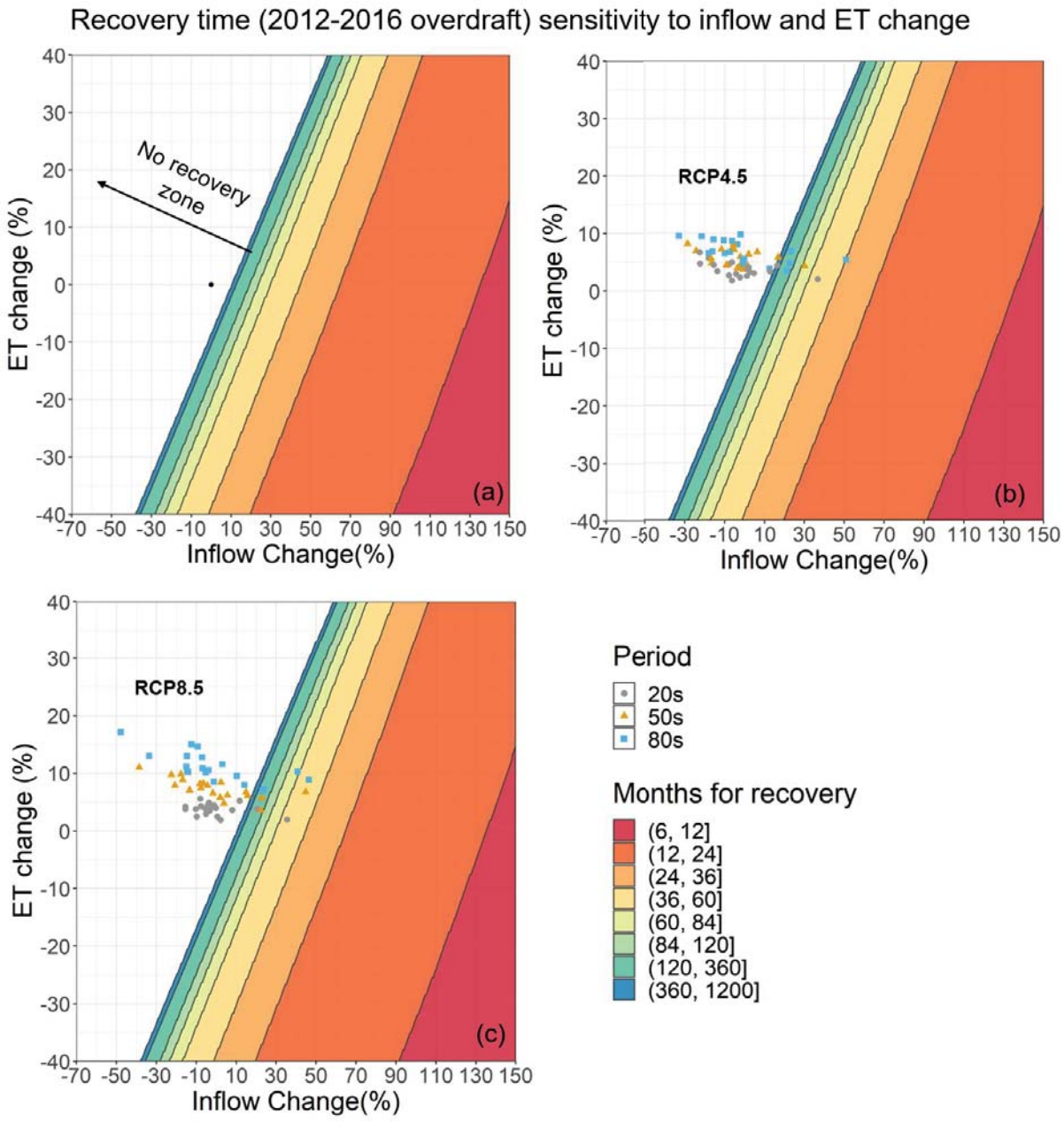
Recovery time (2012-2016 overdraft) sensitivity to inflow and ET change
No recovery zone
RCP4.5
RCP8.5
(a)
(b)
(c)
ET change (%)
Inflow Change(%)
Period
20s
50s
80s
Months for recovery
(6, 12]
(12, 24]
(24, 36]
(36, 60]
(60, 84]
(84, 120]
(120, 360]
(360, 1200]